CHARACTERIZATION OF SILICA GEL-WATER VAPOR ADSORPTION AND ITS MEASURING FACILITY

QIU JIAYOU

NATIONAL UNIVERSITY OF SINGAPORE

2003

CHARACTERIZATION OF SILICA GEL-WATER VAPOR ADSORPTION AND ITS MEASURING FACILITY

QIU JIAYOU

A THESIS SUBMITTED

FOR THE DEGREE OF MASTER OF ENGINEERING

DEPARTMENT OF MECHANICAL ENGINEERING

NATIONAL UNIVERSITY OF SINGAPORE

2003

ACKNOWLEDGEMENTS

The author extends his gratitude and appreciation to **Associate Professor Yap Christopher and Associate Professor Ng Kim Choon** for their enlightening advice, guidance and encouragement throughout the course of research.

He extends his appreciation to **Assistant Professor Chua Hui Tong** for his technical advice and the National University of Singapore for the research scholarship during the course of candidature.

He thanks the Thermodynamics Division and Mr. R. Sacadevan and Mrs. Hung, Master program students Ms. Li Yanlin, Mr. Anutosh Chakraborty for giving him their full support and invaluable assistance throughout the duration of this project.

He wishes to thank all family members for their constant inspiration, love and encouragement.

Finally, the author wishes to express his deepest appreciation to my wife for her love.

TABLE OF CONTENTS

SUMMARY

A new methodology for developing adsorption measurement facility is proposed using a Thermogravimetric Assembly (TGA). This adsorption measurement facility can meet the requirements of the adsorption experiment with a condensable reaction gas such as water vapour. Condensation of water vapor on the measurement system is prevented successfully and the effect of condensation on the isotherms and kinetics is eliminated. Using TGA, the measurement facility measures the sample weight directly and instantly. Adsorption characteristics of water vapor on silica gel were analyzed and compared with those obtained with other systems. In this report, the condensation of water vapor has been prevented successfully within the TGA system at two places: one is supply tube between water vapor supplier and the TGA; another is the upper section of reaction tube. Experimental procedure for this system was also developed based on the experience of running experiments. This system provides a new methodology of dealing with condensable reaction gases for adsorption experiment.

A comparison is made between the experimental isotherms with those obtained with the C.V.V.P (constant volume variable pressure) system.

From kinetic analysis of vapor uptake, the average effective diffusivities of water vapor by silica gel have been determined. Based on the effective diffusivity, an effective temperature, which accounts for real behavior of adsorption in the linear driving force model has been proposed. This new correlation is found to fit the experimental data across a full range of vapor temperature, for which the experiments were conducted.

LIST OF TABLES

LIST OF FIGURES

CHAPTER 2

CHAPTER 3

CHAPTER 4

CHAPTER 5

CHAPTER 6

APPENDIX A

LIST OF SYMBOLS

a	Radius of sphere	m
C	Concentration of adsorbate	kg/m^3
C_0	Constant concentration of adsorbate at the surface of sphere	kg/m^3
C_1	Initial concentration of adsorbate in sphere	kg/m^3
D	Diffusivity	kg/m^2
De	Effective diffusivity	m^2/s
D_{eo}	Pre-exponent constant in the kinetics equation	m^2/s
E_a	Activation energy of surface diffusion	J/mol
K	Adsorption equilibrium constant	---
K_0	pre-exponent constant in the Henry's law correlation/Tóth's law correlation	Pa^{-1}
k_a	Adsorption constant	----
k_d	Desorption contant	----
M_{sg}	Mass of adsorbent in adsorber	kg
M_t	Mass of adsorbate in sphere at time t	kg
M_∞	Mass of adsorbate in sphere at equilibrium	kg
m_{sg}	Dry mass of silica gel	mg
m_t	Total mass weighted	mg
m_{sc}	Mass of sample container	mg
Δm_{sys}	System deviation	mg
n	Equation parameter refer to *Freundlich's* equation	---
	Constant for diffusivity equation	---
P	pressure	Pa
Q_{st}	Isosteric heat of adsorption	J/kg

Q_{total}	Total amount of absorbed heat at evaporator	J/kg
q	fraction of refrigerant adsorbed by the adsorbent	kg/kg of dry adsorbent
q^*	fraction of refrigerant which can be adsorbed by the adsorbent under saturation condition	kg/kg of dry adsorbent
R	Universal gas constant	J/mol K or J/kg K
r	Distance to center of sphere	m
T	temperature	^oC or K
T_{eff}	Effective temperature for diffusivity equation	^oC or K
T_0	Basic temperatue	^oC or K
t	Equation parameter (refer to *Tóth's* equation)	----
□	Surface coverage or fractional filling of the micropore	
u	Adsorbate concentration	kg/m^2
Δq	Amount of adsorbate in adsorption refrigeration	kg
ΔH_{fg}	Latent heat of vaporization	J/kg

CHAPTER 1 INTRODUCTION

1.1 Background

Adsorption occurs whenever a solid surface is exposed to a gas or liquid at a given thermodynamic state. Under a given pressure and temperature, the concentration of adsorbate in an adsorbent, and its total effects depend on the surface of solid and the surrounding concentration of gas or liquid. Ancient Egyptians, Greeks and Romans [1] have discovered the properties of common materials such as clay, sand and wood charcoal, etc. They found that these materials could remove colour from solutions containing dyes, as well as removing unpleasant odours in the air when wood charcoal are used as adsorbent. Although the working principles were not known at that time, it was adsorption that played an important role in these applications.

For several decades, adsorption is found in many applications such as processes involving desiccants and catalysts. For example, the separation of noxious gases for emission control of flue gases or the purification of liquid from a multi-component solutions. A recent important process involving sorption is known as the pressure-swing adsorption where the removal of one component from the main stream fluids could be expedited [2-4]. Heat-driven sorption separation, on the other hand, usually employs waste heat and a common example of this type of application is in the adsorption chillers [5, 6].

Traditional air-conditioning plants employ refrigerants that could cause harm to the ozone layer, where the release of man-made chemicals contains Chlorofluorocarbons (CFCs), bromine and other related halogen compounds and nitrogen oxides. CFCs are alleged to deplete the ozone layer. With the strigent environmental requirements, conventional refrigeration methods have been hard-pressed in facing this challenge. Traditional refrigeration machines use electricity as

the energy input, which is produced by burning the fossil fuels directly leading to CO_2 emissions. As the supply of fossil fuels is finite, new processes with energy-saving potential have become increasingly attractive. Thus, it is important to develop alterative methods in refrigeration in various areas for human safety and economical replacement of CFCs.

There has been increasing usage of the adsorption cycle in the refrigeration over the past decades [5, 6]. Adsorption cooling systems could use the industrial waste heat or renewable sources as the energy input. As such, there is no direct consumption of fossil fuel nor does it consume electricity. Thus, this system saves energy and minimizes environmental pollution. In an adsorption cycle, cooling is generated at the evaporator by the simultaneous vapour (water) uptake and heat rejection of adsorbent (silica gel) in a reactor vessel or bed over a period of operating time interval or cycle time. At the same time, a similar reactor vessel, which contains previously saturated adsorbent, is supplied with a heat source, such as hot water circulation from a waste heat source. The supplied heat purges the adsorbate from the adsorbent in a desorption process. The purged adsorbate flows into a condenser, cooled by water from the cooling tower. The vapour condenses and liquid condensate is flushed back to the evaporator via a u-tube that accounts for the pressure differences in the vessels.

There are many types of working pairs of adsorbent-adsorbate, namely silica gel-water vapour, activated alumina-water vapour and Zeolite-water vapour [7]. Silica gel-water vapour is often used as the working pair in the adsorption chillers. This is because water has a large latent heat of vaporisation and contains no CFCs. Being heat-driven, the adsorption chillers have almost no moving part and, hence, less maintenance is required as compared to the conventional chillers.

From the viewpoint of an industrial design, it is necessary to explore the adsorption characteristics of silica gel-water vapour working pair under different pressures and temperatures. Adsorption measurements have been made on porous materials, in particular, gas adsorption is employed for the determination of the surface area and pore size distribution of porous materials [8]. Adsorption characteristics of silica gel-water vapour are key data for estimating the performance of adsorption chillers and such characteristics include the adsorption isotherm, kinetics and the isoteric heat of adsorption. The adsorption data are useful in the modelling and the prediction of the operation performance of the adsorption refrigeration system.

A survey of literature indicates that there exist two methods of measuring adsorption characterization, namely volumetric method and gravimetric method [9]. Traditionally, volumetric method is used to test the adsorption characteristics at high and ultra-high vacuum. The disadvantages of volumetric method are its indirect measurement and prone to condensation of reaction gas when conditions are not favourable. When dealing with a condensable vapour, experimental results could be doubtful when the system pressure approaches the saturation pressure.

Another approach in adsorption characterization is the themogravimetric method. Thermogravimetric apparatus (TGA) method is preferred method for isotherm adsorption experiments due to its direct and high accurate measurement of vapour uptake onto the adsorbent as well as the ease of operation [10]. The weight of the adsorbent sample is measured directly in real-time during the experiment, whilst the experimental temperature and vacuum pressure are controlled using a PLC based arrangement. When operated with a condensable vapour, there is also possibility of the vapour condensing at unfavourable conditions. As shown in later chapters, one of the

motivations of the current study is to design a suitable facility to arrest the possibility of condensation in the TGA.

1.2 Objectives Of This Study

The first objective of this study is to design an accurate experiment system that can handle a condensable vapour during the adsorption characterization process. The second aim is to determine and analyse the adsorption characteristics of silica gel-water working pair, in terms of the isotherms and diffusion kinetics.

A Cahn TG-2121 adsorption test machine is used for the experiments. The TG-2121 can accommodate a wide range of temperatures (0 ^{o}C to 1100 ^{o}C) and pressures (atmospheric pressure to 5×10^{-5} Torr) [11] and it is suitable for the adsorption characterization. However, it suffers from condensation when a pure vapour is used. Any liquid present in the sample container would render inaccurate weights of recording.

In this thesis, delivery system will be described and tested that could avoid the condensation but provides a continuous supply vapour to the TGA. These systems have been calibrated for operation at the operation ranges of pressure and temperature range from 304K to 358K, and from 800Pa to 6000Pa, respectively, operation conditions that are similar to those found in adsorption cycles.

Chapter 2 describes the literature review of the work on adsorption. It also presents the basic knowledge and terminologies used in the thesis [6].

Chapter 3 describes the properties of silica gel used in the experiment.

Chapter 4 describes the experimental apparatus, including the novel modifications made on a commercially available TGA so that it could handle a condensable vapour with continuous vapour delivery. Chapter 4 also outlines the experimental procedure, results on adsorption isotherms, adsorption kinetics and experimental calibration.

The results obtained from the experiment are discussed in chapter 5. The calibration of experiment and error analysis are included and the correlation of isotherm and kinetics equations are discussed in this chapter.

The conclusion of the thesis is found in Chapter 6 together with the recommendations for future experimental work.

CHAPTER 2 LITERATURE REVIEW

Adsorption refrigeration technologies are becoming increasingly important in industrial applications. One reason is that the adsorption can be driven by low-grade energy, such as the industrial waste heat or the solar energy. A second reason is that the heat-driven chiller has almost no moving parts. These two reasons make the adsorption chillers environment friendly and result in energy saving. Many researchers have completed investigations on principles of adsorption refrigeration with different working pairs [6]. One of the key parameters for adsorption chiller is the adsorption characteristic: that is the amount of vapour uptake by the adsorbent at a given pressure and temperature. This chapter, which consists of two sections, reviews the principle of adsorption, as well as summarizes the adsorption measurement machines.

2.1 Principle Of Adsorption

When a specially treated porous material is exposed to fluid (gas or liquid) at a given pressure and temperature, adsorption occurs as the enrichment of one or more components of fluid on the interfacial layer (surface) between the fluid and the solid material. The adsorbed substance on the solid surface is termed adsorbate and the solid is term adsorbent. There are two different types of adsorption: physisorption and chemisorption. Physical adsorption is due to the presence of Van der Waals forces, which are similar to those responsible for the condensation of vapor or the deviations from ideal gas behavior [8]. Chemical adsorption, on the other hand, involves a reaction between adsorbate and adsorbent resulting in the formation of chemical compounds [6, 9, 12, 13] and this thesis deals with the former. Physical adsorption is an exothermic process where heat is released during the vapor uptake [14]. The isoteric heat of adsorption at normal adsorption working conditions can be higher than the heat of vaporization (condensation) of the adsorbate by as much as 30 to 100%.

2.1.1 Adsorption Equilibrium

For a given temperature and gas or vapor pressure, the gas or vapor would adsorb onto the surfaces of the adsorbent and become adsorbate. The adsorption uptake would increase with time and, eventually, the quantity of adsorbate uptake could saturate and reach a maximum. For a given adsorbent and adsorbate pair, the equilibrium uptake is described, given [13, 15]:

$$q = \mathrm{f}(P,T)$$

where q is the amount of adsorbate adsorbed onto the surface layer per unit weight of the adsorbent, P is the equilibrium pressure and T is the absolute temperature.

Adsorption equilibrium can be expressed in three ways:

(1) When the adsorbent temperature is kept constant and the gas pressure varies, the change in amount of adsorbate against the pressure is called the adsorption isotherm:

$$q = \mathrm{f}(P) \qquad \text{at } T = \text{constant}$$

(2) When the gas pressure is kept constant and the adsorbent temperature varies, the change in amount of adsorbate against the temperature is called the adsorption isobar:

$$q = \mathrm{f}(T) \qquad \text{at } P = \text{constant}$$

(3) If the amount of adsorbate is kept constant, the change of pressure against the temperature is called the adsorption isostere:

$$P = \mathrm{f}(T) \qquad \text{at } q = \text{constant}$$

In adsorption equilibrium study, the adsorption isotherm is often used to express the results of adsorption. In contrast, isobars and isosteres are seldom used to studies of adsorption equilibrium.

2.1.1.1 Adsorption Isotherms

Adsorption isotherms are the changes of adsorbate with varying gas pressure under a constant temperature condition. There are several mathematical models and theories for describing adsorption isotherms but many are essentially empirical approaches in which experimental results are correlated using two or more empirical parameters [8]. Generally, these empirical equations describe the experimental results more accurately than other methods. Different modeling approaches found in the literature include the kinetics, the Gibbs thermodynamic, vacancy solution theory and potential theory approaches.

Many different isotherms may be obtained from experimental data for a wide variety of gas-solid working pairs. However, the majority of physical adsorption isotherms are grouped into six types by the IUPAC (International Union of Pure And Applied Chemistry) classification system, as shown in Figure 2.1 [10]. The first five types (I to V) of the classification were originally proposed by Brunauer et al [9] and type VI was included by IUPAC (Sing et al.) [9, 16].

Type I isotherm is of the classical Langmuir form and is given by a microporous solid having a relatively small pore size. It is concave relative to the pressure axis. It rises sharply at low relative pressure and reaches the limiting value (equilibrium) when relative pressure approaches one. This type of isotherm often happens in micropores with strong interaction, such as activated carbon.

Type II isotherm is concave relative to the pressure axis, then almost flat for a short pressure range and, finally, convex to the relative pressure axis. It indicates the formation of an adsorbed layer whose thickness increases progressively with increasing relative pressure. This type of isotherm often happens in macropores with strong interaction, such as clay.

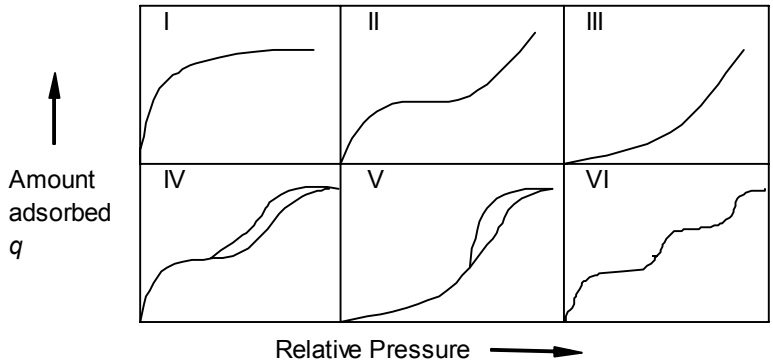

Figure 2.1 The six types of gas physisorption isotherms

Type III isotherm is convex to the relative pressure axis in the full range. It means that the adsorption between adsorbate and adsorbent is very poor. This type of isotherm often happens in macropores with weak interaction, such as Bromine on silica gel.

Type IV isotherm behaves like Type II at the low pressure, and levels off at high relative pressure. This type of isotherm shows a hysteresis loop. This type of isotherm often happens in mesopores with strong interaction, such as Zeolites.

Type V isotherm behaves like Type III at low relative pressure, and levels off at high relative pressure. This type of isotherm shows poor adsorption at low relative pressure and shows a hysteresis at high relative pressure during desorption. This type of isotherm often happens in mesopores with weak interaction, such as water on charcoal.

Type VI isotherm behaves in a manner of step and this is caused by multi-layer adsorption in the micropores of adsorbent.

2.1.1.2 *Langmuir* Adsorption Isotherm

The *Langmuir* isotherm is based on the kinetic theory of gases with emphasis on the thermodynamic and a statistical approach. Kinetic theory assumes that the

adsorption and desorption rates should be the same when the system reaches equilibrium. The *Langmuir* isotherm is based on the following assumptions [8]:

- The adsorption surface is homogeneous,
- Adsorption occurs only at localized sites, and there is no molecular motion,
- Each site can accommodate only one molecule

Assuming that there is a unit solid surface vacancy when the system reaches an equilibrium state, the adsorption rate ($k_aP(1-\theta)$) would be equal to the desorption rate, ($k_d\theta$) [6]. Equating these two rates for the equilibrium condition yields,

$$k_d\theta = k_aP(1-\theta) \qquad (2.1)$$

where k_d is the desorption constant

k_a is the adsorption constant

θ (=q/q^*) is the surface coverage or fractional filling of the micropores

q is the adsorbed phase concentration at equilibrium

q^* is the adsorption capacity of the adsorbent

P is the partial pressure in the gas phase

From Equation (2.1), it can be shown that the Langmuir isotherm is given by:

$$\theta = \frac{KP}{(1+KP)} \qquad (2.2)$$

where K (=k_a/k_d) is the adsorption equilibrium constant.

For low pressures, Equation (2.2) reduces to the linear or *Henry* type equation because the amount adsorbed is far less compared with the adsorption capacity of the adsorbent:

$$\theta = q/q^* = KP \qquad (2.3)$$

where the adsorption is proportional to the partial pressure of gas phase.

When the partial pressure of the gas phase is near to the saturation pressure of the adsorbent temperature, the adsorption amount will reach its maximum for that temperature and all sites are assumed to be occupied [6]:

$$\theta = q/q^* = 1 \tag{2.4}$$

Generally the adsorption amount increases linearly with pressure at low pressure (compared to its saturation pressure). Then the increasing rate gradually decreases as the pressure increases, and the adsorption amount reaches its capacity when the pressure nears to saturation pressure.

The isosteric heat of adsorption is defined as the ratio of the infinitesimal change in the adsorbate enthalpy to the infinitesimal change in the amount adsorbed [8]. When adsorption occurs, heat is released due to adsorption and is partly absorbed by the solid adsorbent, resulting in an increase of the particle temperature. The increasing temperature will slow down the adsorption.

The isosteric heat of adsorption, Q_{st}, is calculated from the thermodynamic *Van't Hoff* equation [6],

$$\frac{-Q_{st}}{RT^2} = \frac{d\ln K}{dT} \tag{2.5}$$

From Eq. (2.5), we can find

$$K = K_1 \exp^{\left(\frac{Q_{st}}{RT}\right)} \tag{2.6}$$

where K_1 is a constant

Substituting Eq. (2.6) into Eq. (2.3), we obtain

$$\theta = \frac{q}{q^*} = K_1 \exp^{\left(\frac{Q_{st}}{RT}\right)} P \tag{2.7}$$

Rearranging Eq. (2.7) gives

$$q = K_1 q^* \exp^{\left(\frac{Q_{st}}{RT}\right)} P \tag{2.8}$$

Taking the logarithm of both sides of Eq. (2.8)

$$\ln\left(\frac{q}{P}\right) = \frac{Q_{st}}{RT} + \ln K_1 q^*$$

$$\text{or} \qquad \ln\left(\frac{q}{P}\right) = \frac{Q_{st}}{RT} + \ln K_0 \qquad (2.9)$$

where $K_0 = K_1 q^*$

By plotting $ln(q/P)$ versus $1/T$, the gradient and intercept yields the Q_{st} and K_0, respectively.

2.1.1.3 *Freundlich's* Adsorption Isotherm

The *Freundlich* equation was an empirical equation used extensively by *Freudlich*. The adsorption amount can be expressed [6, 8, 13]:

$$q = kP^{\frac{1}{n}} \qquad (2.10)$$

where q is the adsorbed phase concentration at equilibrium, P is the partial pressure in the gas phase, k and n are the equation parameters.

This equation is often used to describe the adsorption of organics from aqueous streams onto activated carbon and gas phase system having heterogeneous surfaces with the small range of pressure. The *Freundlich* equation is limited in pressure range, and is normally accurate in small measurement range. When n=1, it approaches *Henry*'s equation.

2.1.1.4 *Tóth's* Adsorption Isotherm

The *Tóth equation* is widely used to describe adsorption without the limitation of pressure range [8]. This equation has the following form:

$$\theta = \frac{q}{q^*} = \frac{KP}{\left[1 + (KP)^t\right]^{\frac{1}{t}}} \qquad (2.11)$$

where P is the partial pressure in the gas phase, θ is the surface coverage or fractional filling of the micropore, K and t the equation parameters

When t is equal to 1, the equation reduces to the Langmuir equation. At low pressures, the equation reduces to the *Henry* equation. At high pressures, the equation approaches saturation limit becomes $\theta = 1$. *Tóth* equation is recommended as the first choice of isotherm equation for data analysis of adsorption because of its simplicity and its correct behavior over a wide range of pressure [8].

2.1.1.5 *Dubinin-Astakhov* Adsorption Isotherm

D-A equation is also often used to describe adsorption isotherm. This equation has the following form [8]:

$$\theta_{DA} = \exp\left[-\left(\frac{A_{pot}}{\beta E_0}\right)^n\right] \qquad (2.12)$$

where $A_{pot}=RTln(P_s/P)$, P/P_s is relative pressure, θ_{DA} is the degree of micropore filling, β is the affinity coefficient, E_0 is the characteristic energy of adsorption, n is a parameter.

2.1.2 Adsorption Isobar

When adsorption of an adsorbent reaches equilibrium, the amount change of adsorbate due to the change of temperature with a fixed pressure is called the adsorption isobar. For a solid-gas adsorption isobar study, an adsorption isobar diagram represents adequately an adsorption-regeneration cycle. In the adsorption cycle, as the pressure is maintained at the saturation pressure of the evaporator temperature, the amount of adsorbate reaches its maximum q^*_A. In the regeneration,

the pressure is maintained as the saturation pressure of the condenser temperature, the amount of adsorbate finally reaches its minimum q^*_D. This situation is illustrated on an adsorption isobar in Figure 2.2 (Dotted lines denote an ideal thermodynamic cycle). During the adsorption-regeneration cycle, the amount adsorbed and temperature change is indicated by curves *a* and *b*, which correspond to the saturation vapor pressure at the evaporator temperature and that of condenser temperature, respectively. The difference of the amount adsorbed ($\Delta q = q_{ads}-q_{des}$) refers to the mass of working fluid that creates a sorption refrigeration cycle.

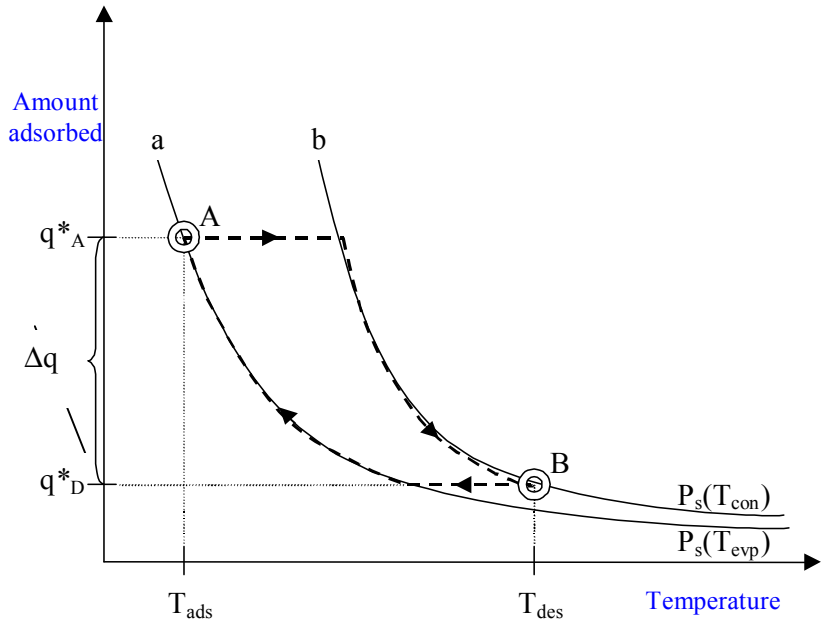

Figure 2.2 Adsorption isobar showing the ideal cycles of adsorption and desorption.

The data from the above diagram is useful for adsorption refrigerator design. During the adsorption stage, the total amount of absorbed heat at the evaporator is represented by the following equation [6].

$$Q_{total} = \Delta q \, \Delta H_{fg} \, M_{sg} \qquad (2.13)$$

where ΔH_{fg} represents the latent heat of vaporization and M_{sg} denotes the total mass of adsorbent. With regard to the mass of working fluid ($M_{sg}\Delta q$), it is clear from the Isobar diagram that T_{des} and T_{ads} are variables when the values of condenser and evaporator's pressures are fixed because the condenser and evaporator's saturation temperatures are decided by the surrounding conditions. The higher the regeneration temperature or lower the adsorption bed temperature, the larger is the Δq. Then the cooling capacity of refrigerator can be increased with the same system. During designing adsorption refrigerator, this diagram can be used as the reference for the selection of system parameters.

2.1.3 Adsorption Kinetics

2.1.3.1 Introduction

In the design of an adsorption cycle, the capacity of adsorbent may be determined from an investigation of the adsorption equilibrium. On the other hand, it is also very important to determine the diffusion of adsorbate into the adsorbent because this process is controlled by the ability of adsorbate molecules to diffuse into the adsorbent particle interior. For a straight cylindrical capillary, there are several types of diffusion [8, 17]:

- Free molecular diffusion (Knudsen): This flow is induced by the collision of gaseous molecules with the pore wall of capillary, where the mean free path is greater than the capillary diameter. Because the driving force is the collision between molecule and wall, the diffusion of each molecule is independent.
- Viscous diffusion (streamline flow): This flow is also called the Poiseuille flow, which is driven by the pressure gradient. All molecules move in the same direction and speed.

- Continuum diffusion: This diffusion is due to the collisions between molecules of different types. This diffusion happens when the mean free path is much less than the diameter of the capillary.
- Surface diffusion: Different molecules have different mobility on the surface of the capillary due to their different extents of interaction with the same surface.

The real solid porous structure is more complex. The simplest picture of accounting for the solid structure is absorbing all structural properties into transport coefficients or into constants of proportionality, such as the tortuosity factor. There are also many other approaches such as that of Monte Carlo simulation [8].

2.1.3.2 Diffusion In A Sphere

For diffusion in a sphere, the equation for the constant diffusion coefficient is described by [18]:

$$\frac{\partial C}{\partial t} = D\left(\frac{\partial^2 C}{\partial r^2} + \frac{2}{r}\frac{\partial C}{\partial r}\right) \tag{2.14}$$

If the surface concentration is constant, and the initial distribution is $f(r) = u = Cr$, equation (2.14) becomes:

$$\frac{\partial u}{\partial t} = D\frac{\partial^2 u}{\partial r^2} \tag{2.15}$$

With the boundary conditions:

$$u = 0\,,\ r = 0,\quad t = 0$$

$$u = a\,C_o\,,\ \ r = a\,,\ \ t>0$$

and initial condition: $u = r\,f(r)\,,\ \ r = 0\,,\ \ 0 < r < a$

where C_o is the constant concentration at the surface of the sphere, a is the radius of the sphere. If the initial concentration of the sphere is uniform with value C_1, and the

surface concentration is maintained at C_o during the adsorption, then the concentration distribution of the sphere with the time is [18]:

$$\frac{C-C_1}{C_0-C_1}=1+\frac{2a}{\pi r}\sum_{n=1}^{\infty}\frac{(-1)^n}{n}\sin\frac{n\pi r}{a}\exp\left(-Dn^2\pi^2t/a^2\right) \qquad (2.16)$$

When r is near to zero, the above equation can be simplified and the concentration at the centre is given as:

$$\frac{C-C_1}{C_0-C_1}=1+2\sum_{n=1}^{\infty}(-1)^n\exp\left(-Dn^2\pi^2t/a^2\right) \qquad (2.17)$$

The total amount of diffusing adsorbate entering or leaving the sphere after time t is:

$$\frac{M_t}{M_\infty}=1-\frac{6}{\pi^2}\sum_{n=1}^{\infty}\frac{1}{n^2}\exp\left(-Dn^2\pi^2t/a^2\right) \qquad (2.18)$$

The detailed derivations of these equations are discussed in Reference 18.

It can be seen that the single factor for fitting the equation (2.17) is D/a^2. For example, at any time t and taking n=3, equation 2.17 can be simplified to:

$$\frac{M_t}{M_\infty}=1-\frac{6}{\pi^2}\left(\exp(-D\pi^2t/a^2)+\frac{1}{4}\exp(-4D\pi^2t/a^2)+\frac{1}{9}\exp(-9D\pi^2t/a^2)\right) \qquad (2.19)$$

2.1.3.3 Surface Diffusivity

The movement of adsorbate on the surface may contribute to the transport of adsorbate into the partile. The mobility is determined by the relative magnitude of the heat of adsorption and the activation energy of migration. The surface diffusivity can be described by the following equation based on the hopping model [6]:

$$D_s=D_{so}\exp\left(-E_a/RT\right) \qquad (2.20)$$

where D_s is the surface diffusivity, D_{so} the Pre-exponent constant, E_a is the activation energy, R is the unversal gas constant and T is the absolute temperature. Surface diffusivity is widely used in simulation of industrial adsorption applications [5, 19- 21].

2.1.4 Basic Adsorption Refrigeration Cycle

Many investigations were done on the adsorption refrigeration [28-34]. Figures 2.3 (a) and (b) show the schematic diagram of a typical adsorption cycle, operating in a batch manners. The roles of evaporator (where vapour is generated) and condenser (where vapour is condensed) are similar to the other refrigeration cycles and will not be elaborated here. During the desorption process, heat is supplied externally, either from a waste heat or renewable energy sources [6], and the pressure within the reactor or bed would increase as the vapour is released into the condenser until it reaches the vapour pressure commensurate with the condensing temperature. On the other hand, when an unsaturated adsorbent is exposed to the adsorbate (vapour), adsorption occurs accompanied by the release of heat due mainly to the isoteric heat of adsorption: vapour is drawn directly from the evaporator by another line, the evaporation results in the cooling of the circulating water. There is no moving part in the adsorption refrigeration system. This makes the adsorption system more reliable and energy saving.

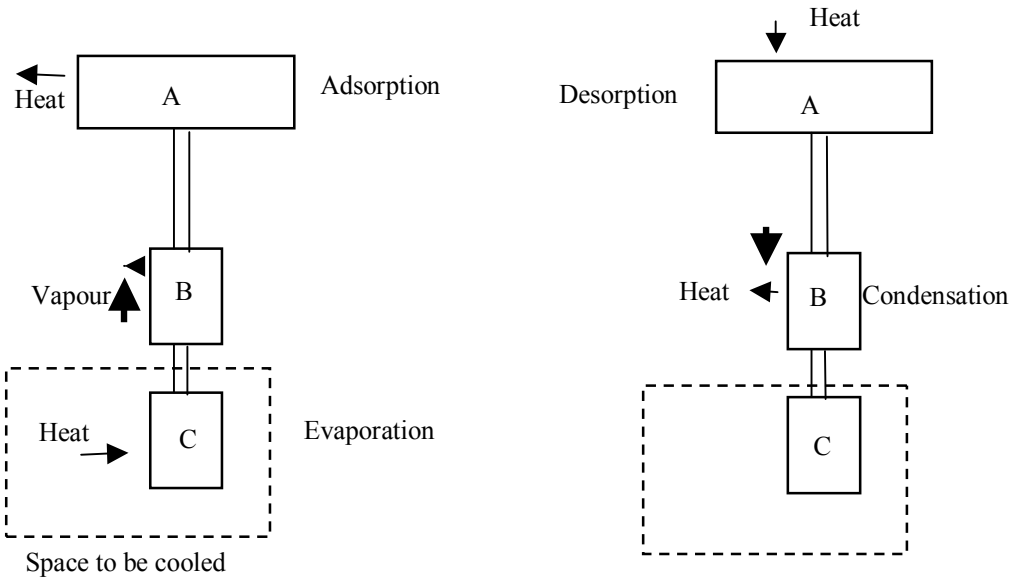

Figure 2.3 Operation principle of closed-type adsorption cooling system: (a) Adsorption cycle; (b) regeneration cycle; A: packed bed of adsorbents; B:condenser; C: evaporator

2.2 Adsorption Measurement Facilities

The aim of adsorption measurement is to determine the properties of the adsorbent-adsorbate working pair, such as the isotherms, adsorption kinetics and adsorption heat data. All these properties are basic information that is helpful for industrial applications. There are several techniques of measuring adsorption data, and many researchers have proposed their machines to measure adsorption [3, 9, 10, 19, 22 and 23]. The two techniques often used are the volumetric and gravimetric techniques. In this section, only adsorption isotherm and kinetics measurement techniques are discussed.

2.2.1 Volumetric Technique

The volumetric technique is based on the pressure change of adsorbate in the constant volume container. Once the vapour is isolated from the system, the total amount of vapour introduced into the chamber is fixed. Due to the adsorption of adsorbent, the pressure of vapour in the chamber or container would decrease. By

tracking the pressure change of reaction gas, the adsorption percentage of adsorbate can be calculated under the measured pressure and temperature during the equilibrium state.

2.2.1.1 BET Volumetric Method

The first volumetric determination was proposed by Emmett and Brunauer and described later by Emmett [24]. The adsorption was measured using a mercury burette and manometer (shown in Figure 2.4). The system is evacuated before experiment. Then, the reaction gas is purged into the volume and the valve is closed after the volume reaches a value. Then, the valve between the volume and the adsorbent is opened. The gas adsorbs onto the adsorbent with the change of volume of reaction gas inside the system. The amount of gas adsorbed is calculated from the change of volume. Then, the isotherm of the adsorbent is obtained. However, mercury burettes are no longer, generally, used because it is more convenient to measure the change of pressure than the change of temperature.

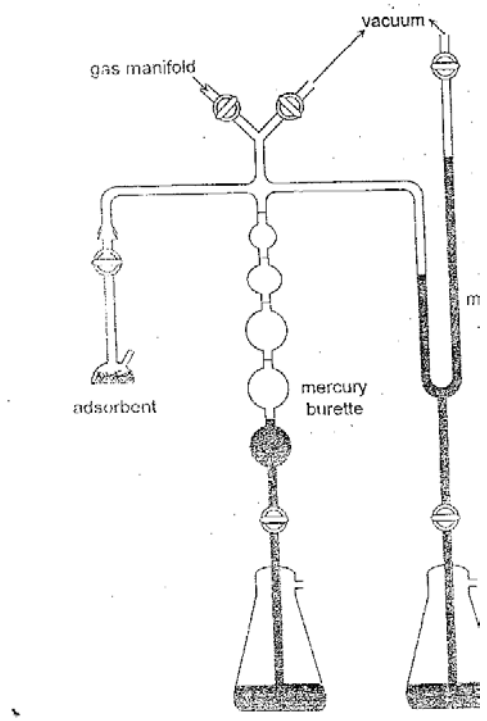

Figure 2.4 BET volumetric method [24]

2.2.1.2 Gas Adsorption Manometry With Reservoir And Double Pressure Measurement

The schematic diagram is shown in Fig 2.5 [25]. The system should be evacuated prior to the start of experiments. The system is isolated from the surroundings by the valve between system and vacuum pump. The amount of gas in the gas reservoir could be obtained with the readings of the first pressure transducer. The valve between system and reservoir is opened when adsorption begins. When the adsorption reaches equilibrium, the second pressure transducer measures the pressure of adsorption equilibrium. The amount of adsorbed gas could be obtained with the pressure difference. It is more convenient to measure the change of pressure than to measure the change of volume. Thus this facility is more direct and convenient for adsorption experiment than the one discussed above.

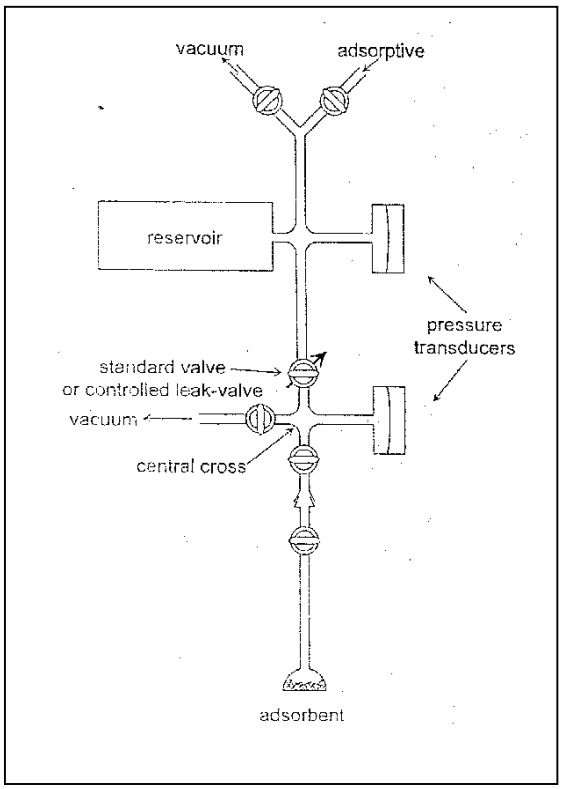

Figure 2.5 Gas adsorption manometry with reservoir and double pressure measurement [25]

2.2.1.3 Differential Gas Adsorption Manometry

The schematic diagram for differential gas adsorption manometry is shown in Figure 2.6 [26]. The adsorptive gas is fed by two carefully matched capillaries into two bulbs (adsorption and reference) from a common reservoir of adsorptive gas. The pressure difference between the two sides provides the amount of gas adsorbed on the adsorbent if the gas flow rates through the two capillaries are the same. The difference between the two downstream pressures should not be too great, or this measurement would not be true. Glass beads in the reaction tube are used to adjust the volume of the two tubes.

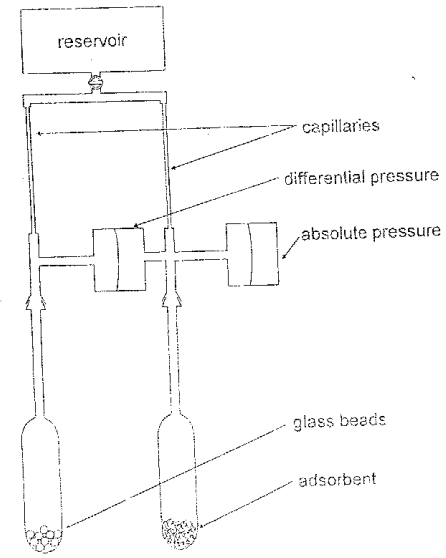

Figure 2.6 Differential gas adsorption manometry [26]

2.2.1.4 Constant Volume Variable Pressure (C.V.V.P.) Manometry

The diagram for C.V.V.P is shown in Figure 2.7 [19]. The system is immersed in a water tank controlled by a temperature bath. Firstly, the reaction gas is purged into the dosing tank from the evaporator, and then the valve between dosing tank and silica gel tank is opened and adsorption begins. The amount of adsorbed gas can be decided from the pressures and volume of dosing tank and charging tank.

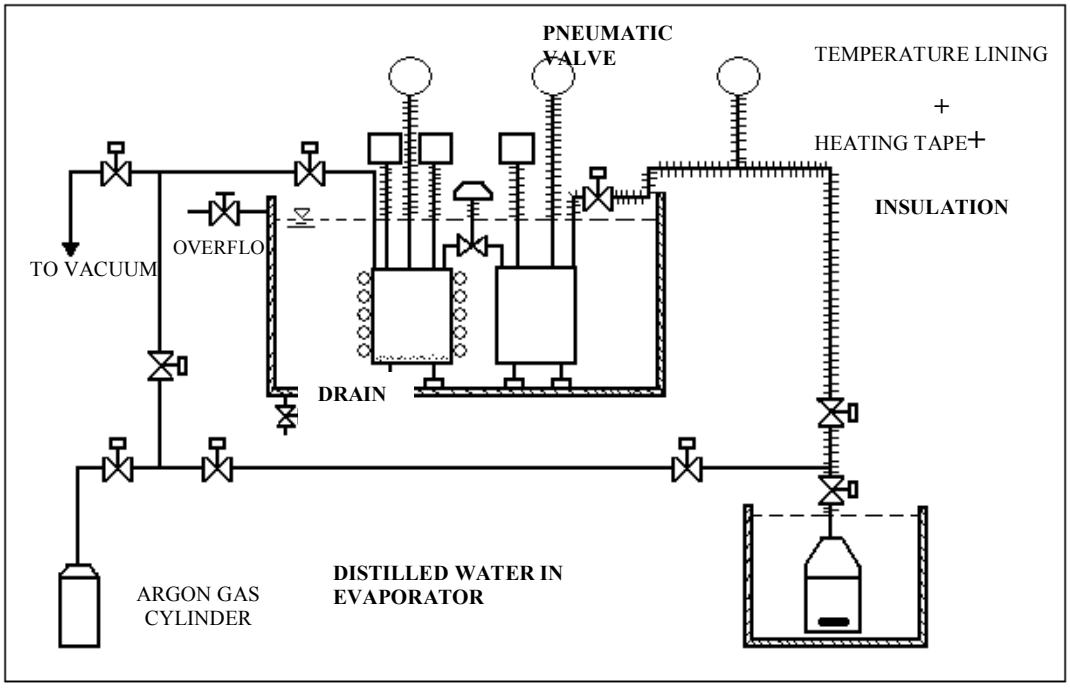

Figure 2.7 Constant volume variable pressure manometry

2.2.2 Gas Flow Techniques

In this approach, a gas flowmeter is used to determine the amount of adsorbate. The set-up is shown in Figure 2.8 [27]. The advantage of this technique is that it could be used for a special type of procedure, For example, the adsorption is the discontinuous point-by-point procedure with a

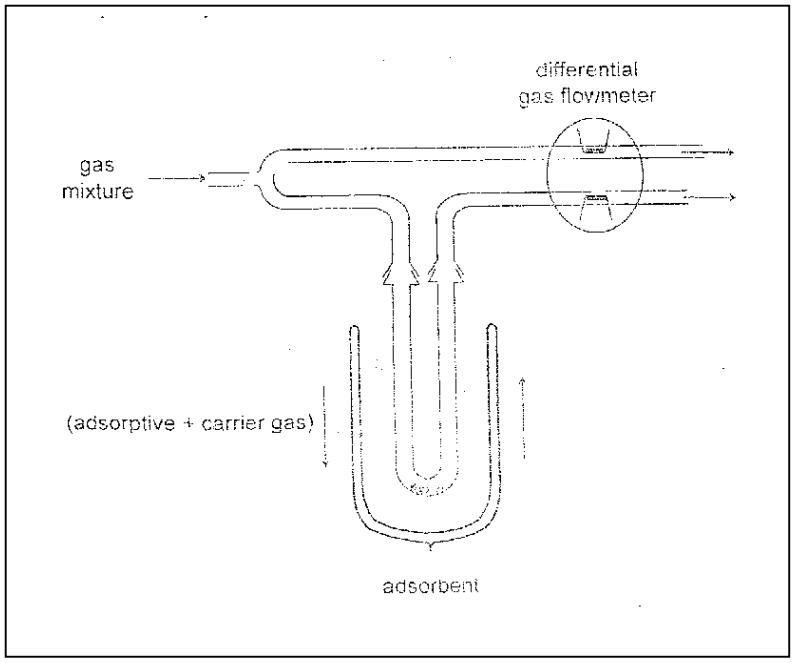

Figure 2.8 Gas flow manometry

non-adsorbable carrier gas. The amount of gas adsorbed is calculated by the integration of the gas flow over a period. Thus great stability and accuracy of flowmeter are essential. The gas flowmeter is used to determine the amount adsorbed.

2.2.3 Gas Adsorption Gravimetry

In gas adsorption gravimetry (Figure 2.9, [22]), the weight of adsorbent is measured directly. Gas adsorption gravimetry is quite suitable for adsorption of condensable vapour because the condensation of vapour on the wall of container will have no influence on the results [28, 29]. However the condensation on the moving balance parts should be prevented, because this will affect the results due to the weight increase by condensation, not by adsorption. The gas adsorption gravimetry can measure the adsorption directly and quickly, but there are also disadvantages, including the buoyancy effect, the need of maintaining the temperature of adsorbent and the electrostatic effect might cause systematic errors.

2.2.3.1 The Gravimetric Methods

The weight of sample is measured by the balance, which is located inside the vacuum system and isolated from the surroundings. The sample is heated by the furnace surrounded. The gas can be purged into the system, and adsorption occurs. The balance measures the weight change of adsorbent directly. Thus the isotherms can be obtained directly at different pressures and temperatures.

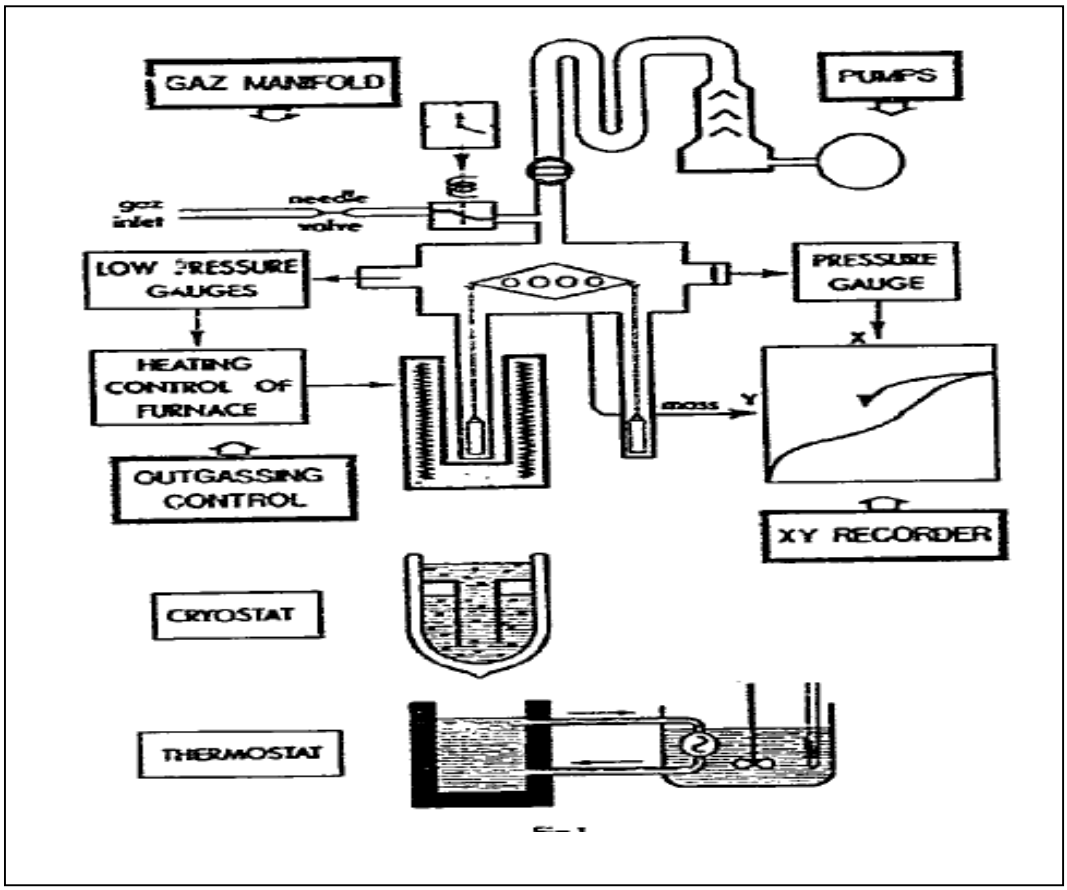

Figure 2.9 Gas adsorption gravimetry

2.2.3.2 Cahn Thermogravimetric Assembly

Cahn Thermogravimetric (TG) is widely used for adsorption analysis for high vacuum and high temperature due to its high accuracy and the ease of control. The sample is weighed using a microbalance. The temperature is maintained by the microfurnace. The system pressure can be lowered to a very low value. The typical TG Assembly (TGA) is shown in Figure 2.10. Cahn TG is only suitable for non-condensable gas adsorption. The details are described in chapter 4 [28].

Figure. 2.10 Cahn thermogravimetric assembly

2.2.3.3. Rubotherm Thermogravimetric Assembly

The Rubotherm TGA is another important product for sorption analysis. The main difference from Cahn TGA is with the use of magnetic suspension couplings for the contactless weighting of samples. The reaction gas enters the system and exits the system from the bottom. Thus it is necessary to make sure that the sample is fully exposed to the reaction gas during experiment. The Rubotherm TG is more concise compared with the Cahn TG. A typical TG is shown in Figure 2.11 [29].

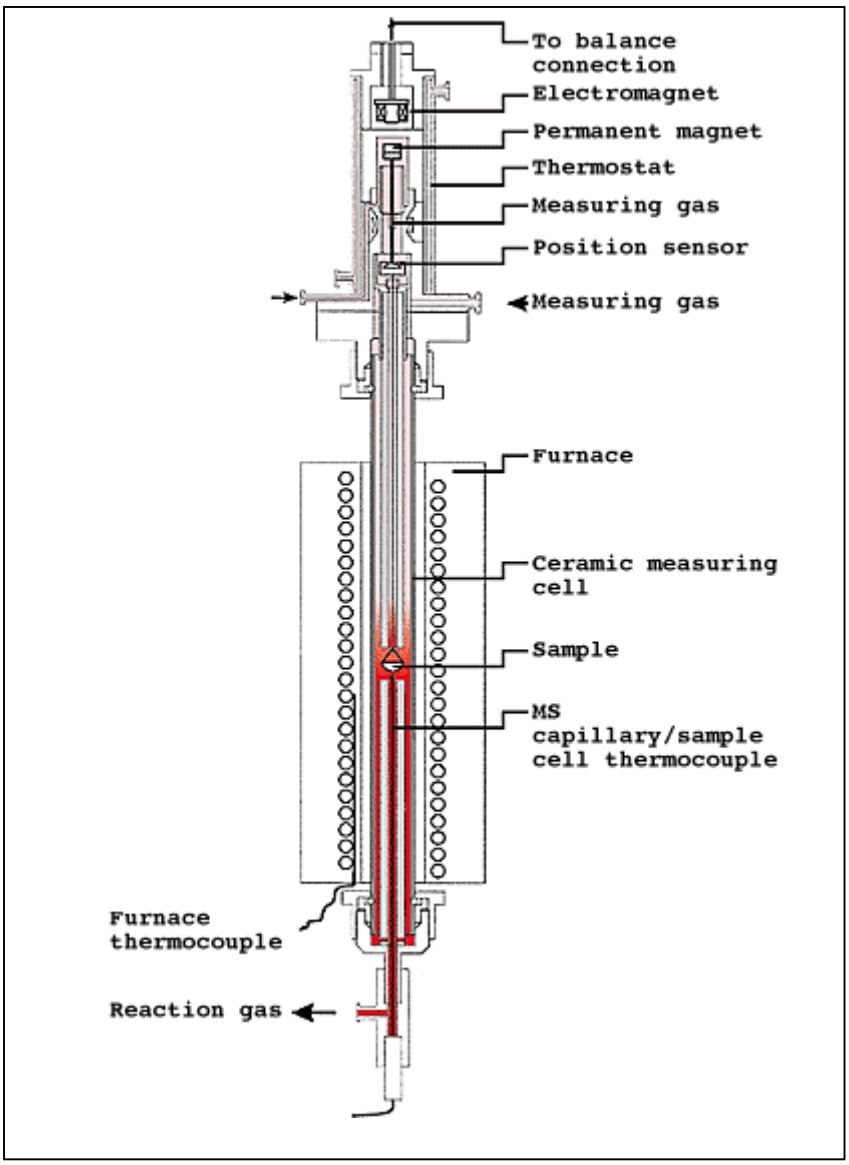

Figure 2.11 Rubotherm thermogravimetric assembly

Currently available technologies to measure adsorption process are presented here. Though these technologies are suitable for adsorption between non-condensable gas and solid, new measurement technology can be developed based on these conventional technologies for some specific purpose.

CHAPTER 3 PROPERTIES OF SILICA GEL

For an adsorbent, it is preferable to have large specific surface area and high polarity. If the specific surface is high, there are more vacancies or places to adsorb the adsorbate. The sizes of these pores determine the diffusivity of the adsorbate molecules onto the surface of adsorbent and, thus, the size and distribution of surface pores are also important properties of adsorbent. On the other hand, if the polarity of adsorbent is high, it is easier to attract the adsorbate molecule onto its surfaces.

Silica gel is one of the most commonly used adsorbents because of its high polar and hydrophilic nature. Physically, it is an amorphous, highly porous, partially hydrated form of silicon dioxide synthesized from sodium silicate and sulfuric acid. It has active and interconnected pores from a vast surface area that attracts and holds water through adsorption and capillary affect, allowing it to adsorb up to 40% (weight/weight) of its dry mass in water vapor. Silica gels are also widely used in industry as filters, catalyst supports, dehydrating agents, air conditioning and refrigeration. Water can be held on the surface of the silica gel by dispersion forces and polar forces as in the case of hydrogen bonding mechanisms.

3.1 The Preparation Of Silica Gel

Silica gel is an adsorbent prepared by releasing silicic acid from a strong solution of sodium silicate by hydrochloric acid under carefully controlled conditions and proportions of liquid sodium silicates and hydrochloric acid [30]. These conditions occur at a reaction temperature and a prescribed pH of the reaction where the mixture is given a finite time for gelling.

The mixture is coagulated into a hydrogel, which is thoroughly washed to remove the sodium sulfate (Na_2SO_4) formed during the reaction. Spherical shaped silica gel particles are prepared by spray drying of the hydrogel in hot air.

3.2 The Physical Properties Of Silica Gel

The silica gels used for this experiment are *Fuji Davison* type 'RD' and type 'A'. The thermophysical properties of this silica gel, as provided by *Fuji Silysia Chemical Ltd., Japan*, and also from [19, 39] are presented in Table 3.1.

Table 3.1. Thermophysical Properties Of Silica Gels *

Property	Type RD	Type A
BET/N_2 surface area [c] ($m^2.g^{-1}$)	838±3.8	716±3.3
BET constant [c]	258.6	293.8
BET volume STP [c] ($cm^3.g^{-1}$)	192.5	164.5
Range of P_r [c]	0.05 ~ 0.23	0.05 ~ 0.19
Pore size [c] (nm)	0.8 ~7.5	0.8 ~ 5
Porous volume [c] ($cm^3.g^{-1}$)	0.37	0.28
Micropore volume [c] (%)	49	57
Mesopore volume [c] (%)	51	43
Skeletal density [d] ($kg.m^{-3}$)	2027	2060
Particle bulk density [e] ($kg.m^{-3}$)	1158	1306
Surface area [f] ($m^2.g^{-1}$)	720	650
Average pore diameter [f] (nm)	2.2	2.2
Porous volume [d] ($cm^3.g^{-1}$)	0.4	0.36
Apparent density [f] ** ($kg.m^{-3}$)	700	730
Mesh size [f]	10 ~ 20	10 ~ 40

PH [f]	4.0	5.0
Water content [f] (mass %)		<2.0
Specific heat capacity [f] ($kJ.kg^{-1}.K^{-1}$)	0.921	0.921
Thermal conductivity [f] ($W.m^{-1}.K^{-1}$)	0.198	0.174

* Manufacturer's representative chemical composition (dry mass basis):
SiO_2 (99.7%), Fe_2O_3 (0.008%), Al_2O_3 (0.025%), CaO (0.01%), Na_2O (0.05%).
[c] Remarks ASAP 2010. [d] Remarks AccuPyc 1330. [e] Remarks computed.
[f] Remarks Manufacturer. ** This value is inclusive of bed porosity.

3.3 Adsorption Characteristics Of Silica Gel-Water Vapor

The adsorption characteristics of water vapor on silica gel are fundamental data for the design of adsorption refrigeration systems. The characteristics of adsorption may be essentially described by the adsorption isotherms and kinetics. Investigations on the adsorption isotherms [3, 5, 19, 32, 33] and adsorption kinetics [3, 31, 34-36] have been reported. The details of adsorption isotherms and kinetics of silica gel-water vapour will be discussed in Chapter 5.

3.4 Regeneration Of Silica Gel

3.4.1 Introduction

For industrial applications, the adsorbent is used repeatedly for many cycles. When an adsorption process is saturated, it is regenerated so as to prepare the adsorbent for use in next cycle. There are two objectives for the regeneration of adsorbent. The first is to restore the adsorption capacity of saturated adsorbent and the second is to recover valuable adsorbate from the adsorbent. Several alternative methods for the regeneration of an adsorbent have been used, such as the desorption by thermal swing, desorption accomplished by pressure swing, purge gas stripping and displacement desorption. Each mode of regeneration is selected based on technical considerations [4].

3.4.2 Methodology

In this experiment, the Cahn TGA-2121 TGA is used to measure the regeneration process of silica gel. The data during the regeneration is recorded for Type 'RD' and Type 'A' silica gel with respect to temperature and time. The silica gel in furnace is heated up from room temperature of 296K up to 413K and the temperature is maintained for 48 hours under vacuum. Figure 3.1 shows a typical regenerative process of silica gel type RD. The final temperature of regeneration is set at 140°C which was achieved in 200 minutes. Correspondingly the mass of the adsorbent (silica gel) sample drops quickly. To achieve the final dry mass, the 140°C was maintained for 48 hours. The dry mass of silica gel is then determined after this regeneration process.

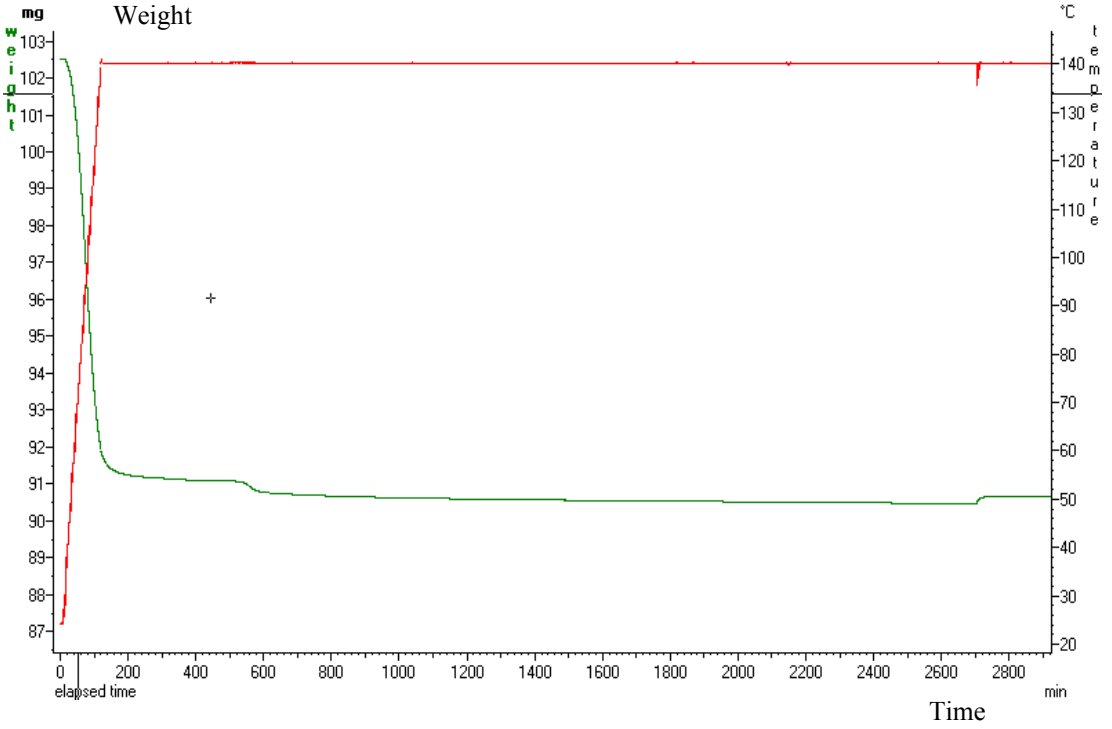

Figure 3.1 Typical temperature-time trace for the regeneration of type RD silica gel for 48 hours

CHAPTER 4 EXPERIMENTAL SETUP AND PROCEDURE

There are many methods used for measuring the adsorption uptake of an adsorbent and the most widely reported procedures are the adsorption isotherm and kinetics. Some of the experimental apparatus used in adsorption studies can only handle non-condensable vapours. However, adsorption of a pure vapour could have the effect of condensation at a certain thermodynamic state during the vapour uptake. Due to the effect of the condensation of vapour, condensation would cause erroneous readings of vapour uptake and should be avoided in such adsorption measurements.

4.1 Introduction

The Thermogravimetric assembly (TGA) method is often used for isotherm adsorption experiments due to the high accuracy, ease of control of the pressure and temperature of the experiment. TGA gives a direct measurement of the quantity of adsorbate adsorbed throughout the uptake process. A microbalance device is used where the adsorbent mass is measured as a function of temperature and time.

In the TGA, the sample container is suspended on an extension wire that is connected to the microbalance. A small furnace is used to provide an isothermal environment for the sample container whilst a temperature sensor measures the temperature of the chamber.

There are two ways to measure adsorption. For example, a gas can be introduced into the TGA system directly, such as TG-2121 series machines. When a condensable vapor is involved, the TGA system faces the problem of condensation. If the temperature of any part of the system is less or equal to the saturation temperature at the experimental pressure, condensation would occur leading to the errors in experimental measurements. To prevent the condensation, the TGA system is often put

in a large container, where the temperature of container is maintained well above that of the condensation temperature. Depending on this method, the whole experiment facility using TGA was heated by heat coils to prevent condensation. For this kind of insulated apparatus, it is clumsy when accessibility to the adsorbent chamber is needed during the experiment.

In this thesis, a TG-2121 is used for the adsorption experiment. The TGA is connected to a new water vapor supplier system which has been designed specially for the requirements of the variable pressures and temperatures. Condensation could be also prevented successfully with the high accuracy of result.

4.2 Modification Of Instrument

The original TG-2121 system was mainly designed as a microbalance but it was unsuitable to a pure water vapour uptake at low vacuum. Thus, it is necessary to modify the TG-2121 to meet the new requirements of the experiments.

4.2.1 Modification On Water Vapour Supply System

Figure 4.1 shows the original design from the manufacturer [11]. A stainless steel mesh or sieve is placed near to the bowl or crucible containing the sample adsorbent. This design is meant for a system with large environment superheat where evaporation of vapour could be easily controlled. However, for tests at a low temperature environment (less than 100 ^{o}C), the sieve method is not effective. The vapour for adsorption has to be introduced using a pumping system where the vapour is generated externally. Figures 4.2 (a) to (c) show the modified TGA system that compromises the following novel designs: (a) an external vapour generator with an independent temperature controller (Hakke® temperature bath) for vapour generation (Figure 4.2 (a)). (b) A heated and insulated flexible hose between the bath and the reaction tube of TG-2121 (Figure 4.2 (b)). (c) A vacuum pump system with a pressure

controller (Figure 4.2 (c)). The schematic diagram of the new design is shown in Figure 4.9.

Before --- Downstream layout circle in red

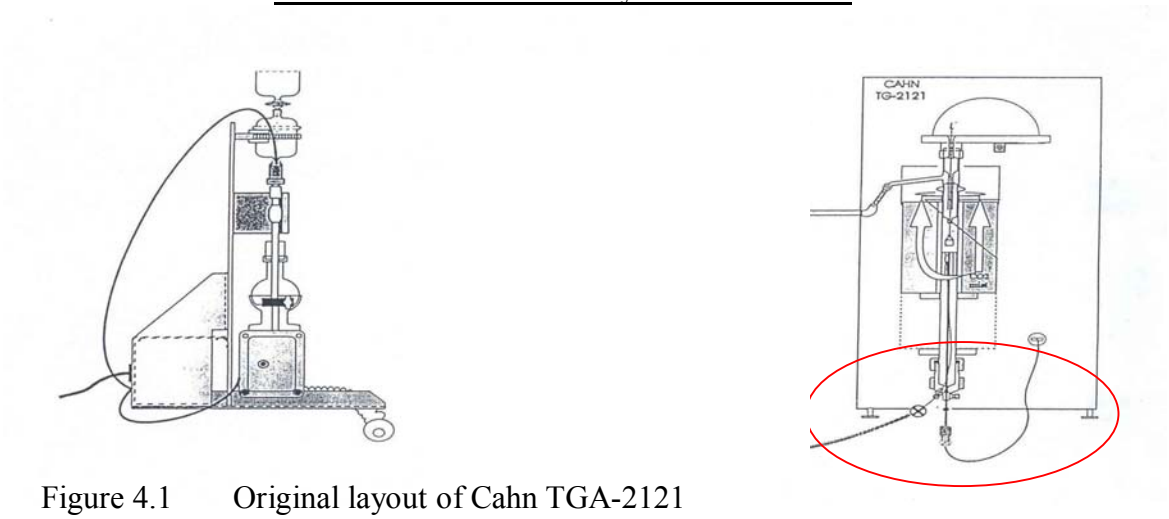

Figure 4.1 Original layout of Cahn TGA-2121

After --- New layout structure

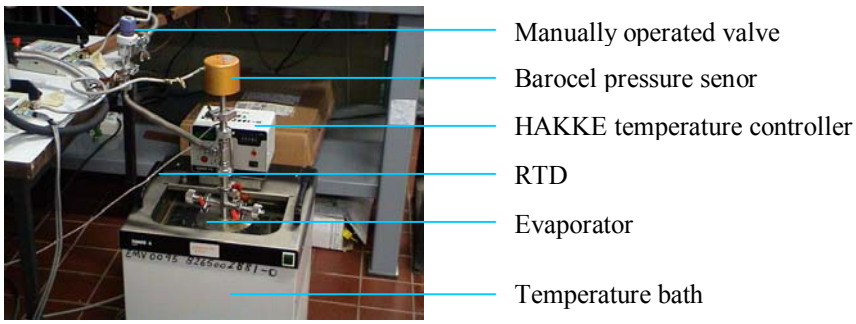

Figure 4.2 (a) A new water vapour generator.

Figure 4.2 (b) Flexible hose between evaporator and reaction tube

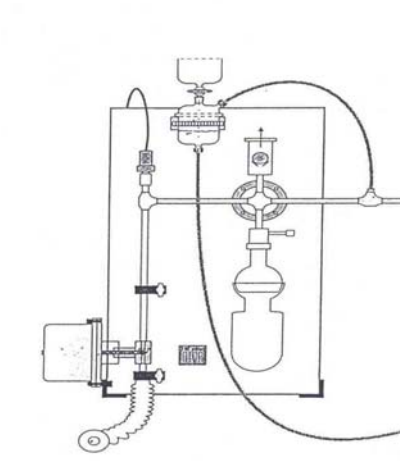

Figure 4.2 (C) Vacuum system with pressure controller

In the above design, calibrated capacitance manometers (Edwards® barocel type 600) and Pt 100Ω Class A resistance temperature detectors (RTDs) are used to measure the vapour pressure and vapour temperature in the evaporator, respectively. A calibrated Hewlett-Packard® (HP) 34970 A Data Acquisition/switch unit (Figure 4.3) continuously monitors all the pressure and temperature readings incorporated within a computer that is responsible for data capturing and processing.

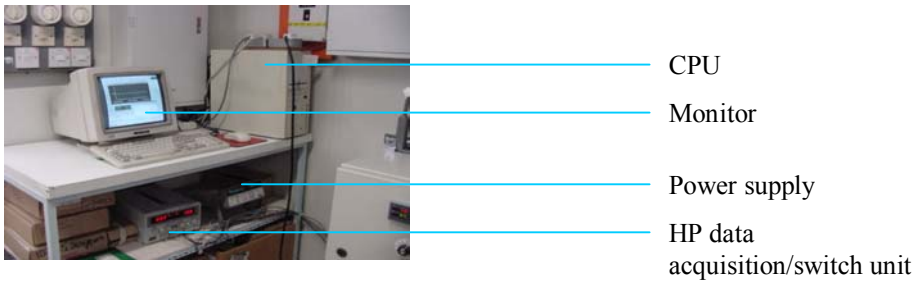

Figure 4.3 HP data acquisition/switch unit

For accurate measurements during the adsorption experiments, the following parameters are measured:

(i.) The vacuum in the reaction chamber is measured by a capacitance manometer (Edwards® barocel type 600). It has high accuracy of from 0 Pa to 1000 Pa, and can be used in an environment less than 0 ^{o}C. Calibration is performed in accordance with standards on a yearly basis.

(ii.) The vapour temperature in the reaction chamber is measured by a resistance temperature detector (RTD 100Ω) of Din accuracy. Calibration is performed in accordance to within ±0.1 ^{o}C.

(iii.) The vapour uptake is measured by the TG-2121 microbalance. It has an accuracy of ±0.1μg.

4.2.2 De-condensation Of Water Vapour

Condensation in the measuring system leads to the error in the experimental data. Special precautionary measures are necessary to prevent condensation of water vapour in the system. At first, an isopad flex type heating tape (220V, 99W, 1.7m) was used to coil around the flexible stainless pipe between the evaporator and TGA with a thermostat (Figure 4.4). This method prevents condensation, but the fluctuation range of water vapour temperature is found to be large and the flow rate of water vapour also fluctuates widely.

To improve the temperature control, a *Reach*® micro processor temperature controller is used, as shown in Figure 4.5, making use of solid state current relay to control the heat tape temperature using a feedback control. The heating tape temperature is initially maintained at about 8K higher than the evaporator temperature to prevent condensation before water vapour is purged to TGA system. All exposed piping, fittings and valves are well insulated by Rubaflex® M1-NF Class O flexible thermal insulation. This further protects the system against condensation and heat losses are avoided.

Figure 4.4 Heating tape with thermostat controller

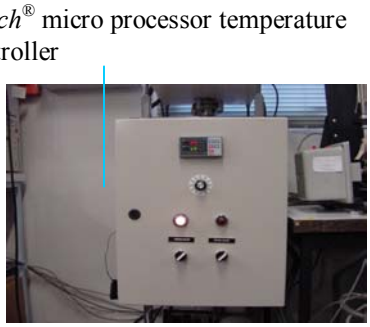

Figure 4.5 Heating tape with *Reach*® micro processor temperature controller

The sample bowl is lifted by a hangdown wire that is hung from the microbalance, and the hangdown wire is protected from condensation of the pure vapour by the injection of helium gas into the protective dome of the microbalance and the top of the reaction tube. Since the baffle tube is filled with helium gas, the outside of the baffle tube is exposed to the water vapour. At low temperatures of wall of baffle tube, condensation may occur that leads to the experimental error. A halogen lamp is placed to radiate energy directly through the reactor tube so as to prevent any condensation on the outer surface of baffle tube.

4.2.3 Pressure Sensor

The position of the pressure sensor is also crucial for the minimization of experimental errors. It is found that the best location for the pressure sensor is under the reaction tube.

4.3 Experimental Setup

With the above-mentioned modifications, the TGA system could meet the basic requirements of adsorption experiments that employ a condensable vapour. Figure 4.6 shows the overall photograph of the TGA apparatus and Figure 4.9 is the schematic diagram of system. The system can be classified into three main portions:

(i) The TGA (Cahn TGA-2121)

(ii) The pressure control system.

(iii) The water vapour supply system.

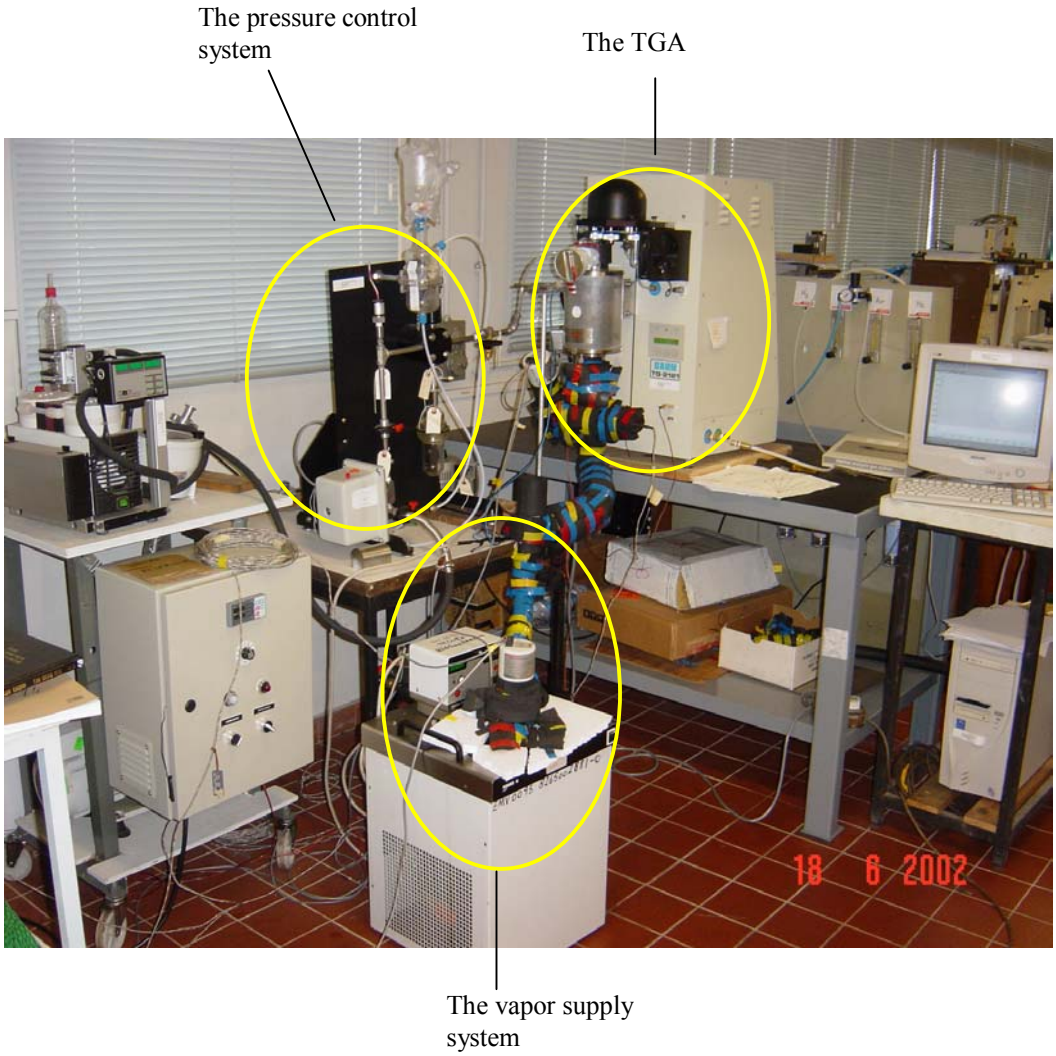

Figure 4.6 Overall view of experimental layout

4.3.1 The TGA

The TGA includes a stand, micro-balance, micro-furnace, status and control panel, thermal gas analysis station, computer and monitor. The details on the different parts are discussed in the following sections.

The stand of the TGA is to provide space for the installation of each component. The instrument stand is designed to be rigid and yet to occupy the minimum space.

The micro-balance measures the weight of sample and it can detect weight changes of the sample in a very short time. Its measurement ranges are between 0 to 150mg with readability up to 0.1μg.

The control panel displays control the functions of the microfurnace, balance and thermocouple and a Pentium computer with an EGA/VGA monitor is connected to the TGA's thermal gas analysis station. Cahn's TGA software in the computer can be used to control operation of the TGA. During the experiment, the time, weight and temperature are recorded continuously at defined intervals and the data are stored on the computer's hard disk [11].

The position of microfurnace is controlled electronically to ensure correct positioning of the sample bowl and the final reading of its mass. The furnace elevator is controlled from the status and control panel of the TGA. Motorized furnace movement allows easy access to the sample container during loading and unloading. The microfurnace can be maintained at temperatures up to 1100°C, with maximum heating rate of 100°C/min, maximum cooling rate of 50°C/min and temperature repeatability of 3°C [11].

A 'K'- type thermocouple, located few millimetres (normally 6 mm) below the sample container, detects and measures the temperature inside the furnace and immediately updates the temperature display both on the status and control panel and monitor screen. Although the adsorbent is not in direct contact with the thermocouple, it is used to read a representative temperature inside the microfurnace. And it is claimed to read the temperature of adsorbent accurately. The distance between the thermocouple and the sample bowl should be small enough to ensure the accurate temperature measurement.

There are two gas inlet ports at the right side panel of the TGA: one is connected to the microfurnace, another is connected to microbalance. A purge gas, namely Helium, is sent into the microbalance so that the balance chamber can be continuously flushed with an inert gas with a purity of 99.9995% (kg/kg). A correct volume flow rate is crucial to achieve gas flow separation [11]. During the experiment, the water vapour from the evaporator flows in an upward direction whilst the helium gas flows in the opposite direction protecting the microbalance. A well-tuned system would achieve a critical balance of gas filled environment above that of the sampling chamber. In the experiments, the rate of the flow of Helium is about 200 ml/min.

To achieve a better control of temperature within the reaction tube, an external source of compressed air is purged into the furnace chamber via two ports in the bottom of the furnace. The air flowing through the furnace chamber and controlled by air regulator provides a heat sink for the TGA-2121 temperature control [11] and it also prevents condensation on the reaction tube.

When the sample is replaced, great effort should be taken when handling silica gel, ensuring no physical contact to prevent the effect of static electricity. The sample container is placed inside the reactor tube, which is suspended by an extension wire and must not exceed the range of the furnace heat zone, as illustrated in Figure 4.7, to ensure an even temperature distribution. It is also important to balance between the sample and tare sides and record the very small weight changes. Normally, the same sized containers are equally used on both sample and tare sides.

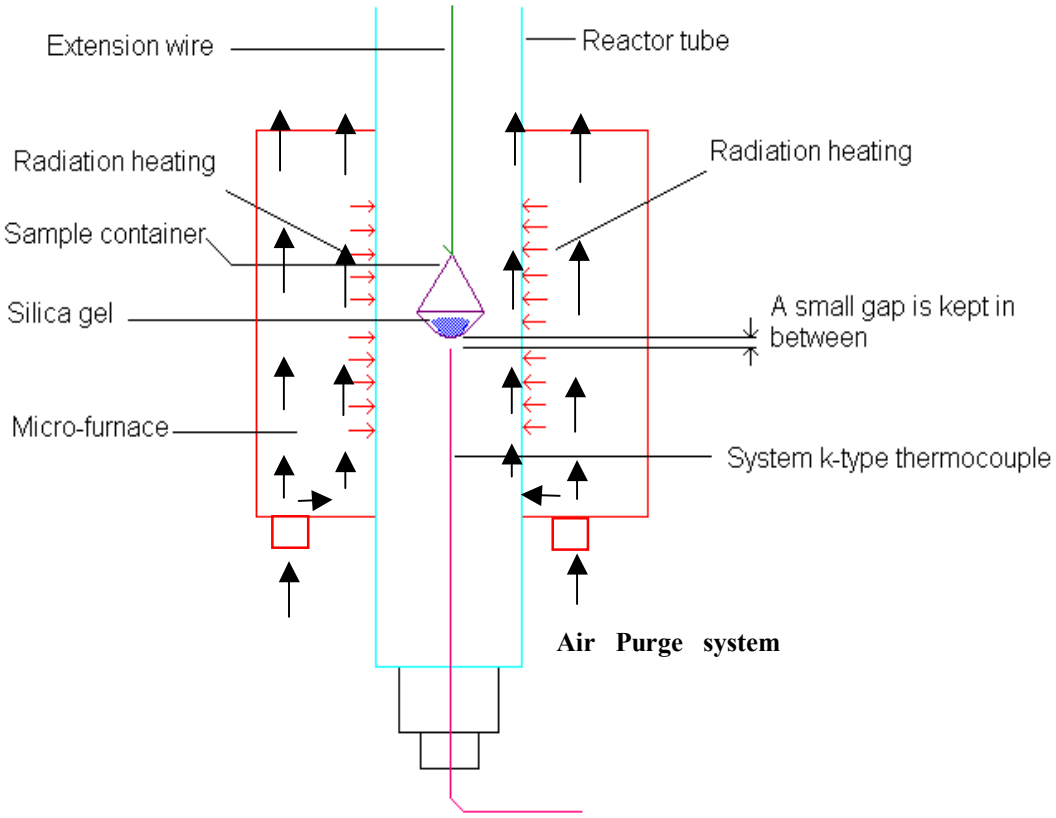

Figure 4.7 Close-up view of extension wire, reactor tube, sample container and thermocouple

4.3.2 The Pressure Control System

A pressure control system is used to maintain low vacuum within the reaction tube and to enable the equilibrium of flow separation between water vapour and helium in the reaction tube. As shown in Figure 4.9, vacuum is affected by the pressure transducer, throttle valve, vacuum pump and a water container. The outlet of the upstream reactor tube is connected to the vacuum line, inter-linked with the throttle valve and vacuum pump. The KNF® vacuum pump would modulate the valve continuously so as to maintain a desired vacuum level of system, which can be set to any desired figure, and the feedback for the throttle valve is from the pressure transducer located at the bottom of reaction tube. The vacuum pumping system consists of a rotary vane vacuum pump (pump type: N842.3 FT.18) with a water vapour pumping rate of 0.57 l/sec at atmospheric pressure. An ultimate vacuum

absolute pressure equal to or less than 200Pa is used to evacuate the system. In compensating for the condensation of water vapour after the outlet of reaction tube, there is a water reservoir to store the water that is accumulated.

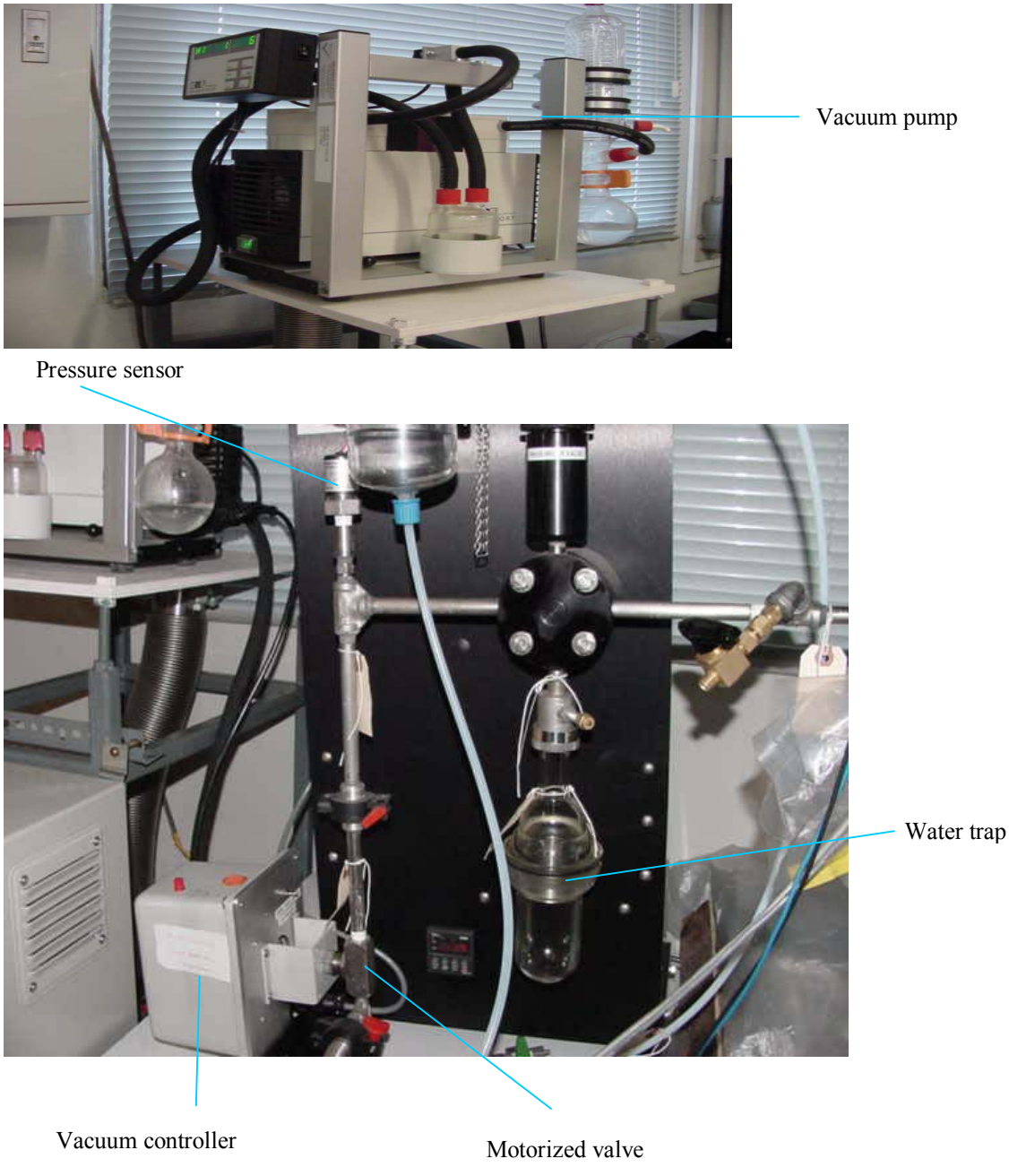

Figure 4.8 The pressure control system

4.3.3 The Water Vapour Supply System

The water vapour supply system to the TGA consists mainly of a temperature bath, an evaporator and heating tape temperature controller, as shown in Figures 4.2 (a), 4.2(b) and 4.2(c).

In order to maintain a constant temperature in the evaporator which is filled with distilled water and immersed in a water temperature bath., a HAKKE® Temperature-Control (precision of control: ± 0.1K) system is used for precision control. The bath temperature can be regulated to supply water vapour at any desired pressure, and the flow rate of water vapour into the TGA can be maintained at a constant value (because the pressure difference between the evaporator and reaction tube is constant).

There is an inter-connecting manually-operated valve with bellow feed through type VAH016-A (INFICON) between the evaporator and the inlet section of reaction tube to allow isolation from water vapour into the TGA system, if needed.

Pipes between the evaporator and the microfurnace are all wrapped with a flex type heating tape along the flexible stainless steel piping. The heating tape is used to keep the wall temperature of the piping higher than that of water vapour to reduce any condensation of water vapour. Other connection pipes, such as the pipe between the pressure transducer and the bottom of the TGA, are also wrapped with the heating tape for the same purpose. The weight change of adsorbent during the experiment will not be affected as condensation of water vapour is prevented in test zone. The temperature of the heating tape is controlled by a micro processor temperature controller type PAK-600 with feedback from the RTD (as mention in section 4.2), which measures the wall temperature of the pipe between the control valve and evaporator.

All inter-connected piping and stainless steel vacuum fittings used are 12.5 mm size. To reduce the measurement error caused by a temperature gradient along the exposed piping, fittings and valves, they are all well insulated. This can also help to prevent condensation along the pipes. Next, to prevent air leak, the O-rings in clamp are placed carefully and seated between joins. Experience shows that both outgassing of non-condensable gases can cause poor vacuum performance and moisture presence is very difficult to be removed from the TGA system.

The temperatures of the evaporator and the bottom of reactor tube in specific point are measured using Pt 100Ω Class A resistance temperature detectors (RTDs).

Likewise pressure inside the evaporator is measured using a calibrated Edwards® Barocel type 600 capacitance manometer. This has an operating temperature range from 0°C to 65°C and a full span of 100kPa with an accuracy of 0.15% of the reading. The pressure of the bottom of reactor tube is measured using a MKS® pressure transducer, which is also the feedback source for the pressure controller system. It is observed that the diameter of the reaction tube is sufficiently large to render the flow rate to be small during the experiment. The pressure difference across/between the bottom of the reaction tube and the test zone is also small and the pressure reading recorded here is nearly the same as that in the test zone.

A calibrated Hewlett-packard® (HP) 34970 A Data Acquisition/switch unit continuously monitors all the pressure and temperature readings. It is used together with the HP® Benchlink Data Logger software [37].

Lastly, to prevent measurement error due to upstream condensation, a halogen lamp, 230V, 50W provides direct radiation energy upstream of the reactor tube (as shown in Figure 4.7).

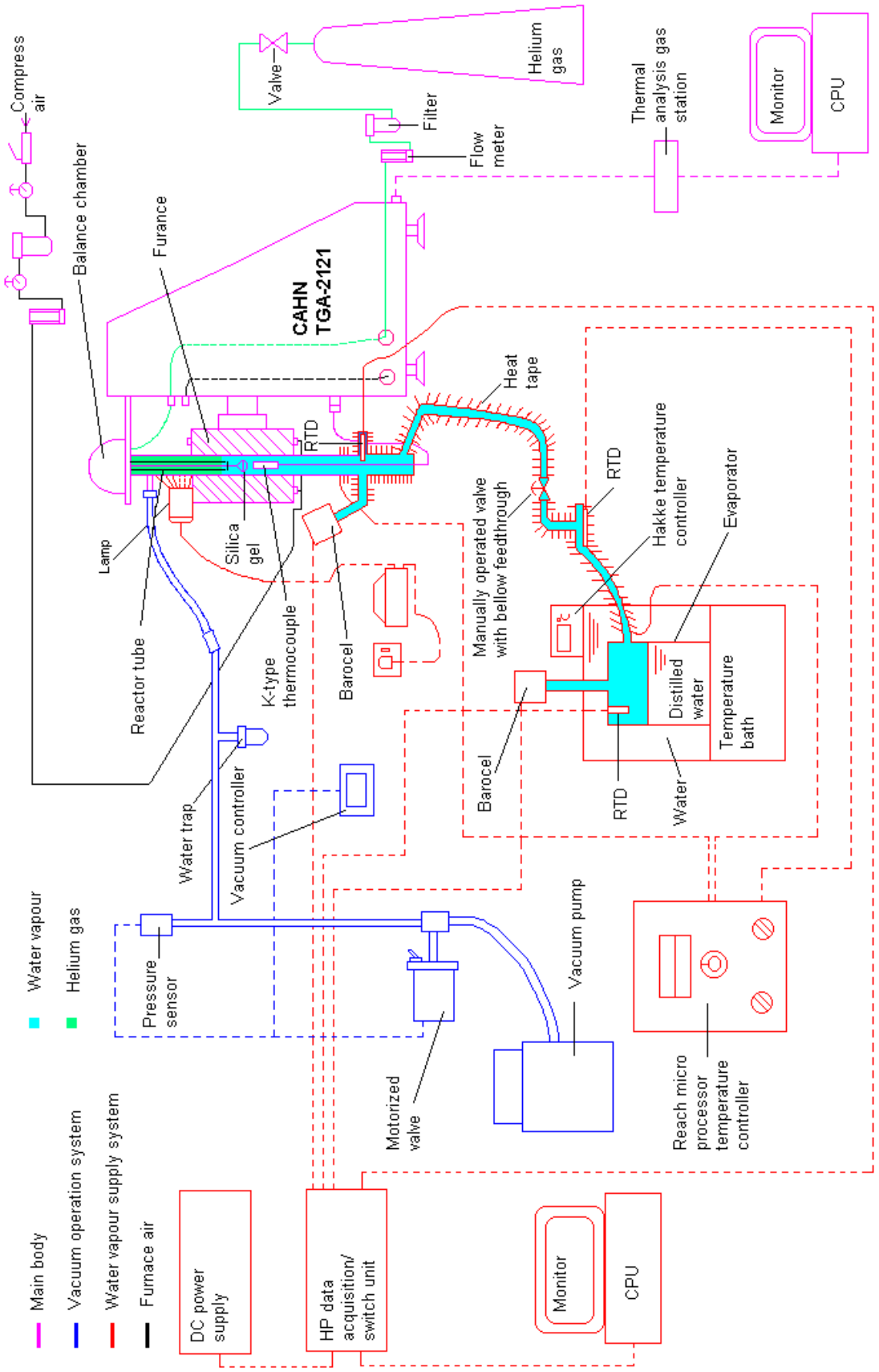

Figure 4.9 Schematic diagram of experimental setup

4.4 Experimental Procedure

The effect of static electricity on the measurement of microbalance is prevented before starting the experiment. Static electricity could accumulate in the baffle tube, hangdown wire and sample bowl in TG-2121 and may be eliminated by wiping with a wet tissue. Silica gel is placed into the sample bowl in the reaction tube, which is located inside the TG-2121 furnace. The hangdown wire is monitored for its concentricity within the baffle and reaction tubes before and after the furnace returns to the correct position. Before the experiment, the evaporator is filled sufficiently with distilled water. To prevent leakage during the experiment, checks to all connections of the experiment facility are made before starting the experiment.

The program for the TGA is set to a desired temperature and a heating rate, and the TGA is set to run. When the temperature of the furnace reaches the desired temperature for more than 30 minutes, the helium gas is introduced into the microbalance at a rate of 100 to 200 ml/min. This is to prevent water vapour from entering the microbalance.

The temperature of bath is set to 5 degree Celsius or lower in order to cool evaporator. The heating tape and halogen lamp are also switched on. After the desired temperatures of evaporator and heat tape are reached, the valve between the evaporator and reaction tube is opened (to ensure that the pressure of the reaction tube is atmospheric pressure, so that shock on the microbalance due to the pressure difference between the evaporator and the reaction tube is avoided). Then, the vacuum pump is turned on to evacuate the whole system. After the pressure of the system reaches 8 mbar or less, the valve between the evaporator and the reaction tube is closed. Subsequently, the whole system is evacuated to remove any traces of condensed water vapour in the system to reduce experimental error. The pressure of the system is then

set to the value for the experiment using the pressure controller. It is also necessary to adjust the voltage for the halogen lamp periodically to ensure that the temperature of the upper part of reaction tube is less or equal to the temperature of the furnace. The temperature of heater tape should be also less or equal to the temperature of furnace. The temperature of hot water bath is adjusted so as to supply water vapour at the measured pressure corresponding to the saturated vapour pressure of water. This temperature is slightly higher than the saturation temperature corresponding to the experiment pressure.

After the temperature and pressure of the furnace are stable and maintained for more than 30 minutes, the inter-connecting valve is opened, the water vapor in the evaporator is purged into the TG-2121 apparatus and the adsorption begins. From prior experience, for safety reasons the inter-connecting valve is opened slowly to release the residual pressure in the evaporator. This is to reduce the spurting disturbance resulting from vapour in various parts of the test system. It is noted that the accuracy can be strongly impaired by the presence of vapour in the microbalance. Steady density and temperature can be maintained after all parts of the system have been purged for some time. When the weight of the adsorbent reaches its largest value and is maintained for more than 30 minutes, adsorption equilibrium is deemed to have been achieved. In preparation for the subsequent run, the inter-connecting valve is closed and the test system is evacuated again. Then the system is set to another pressure value, when the pressure and temperature become stable, the steps discussed above are then repeated.

After the experiments are completed, the program is stopped and the inter-connecting valve to the evaporator is closed. The system is evacuated further by the vacuum pump to prevent any water vapor in the system. The valve between the TGA

system and evaporator is then closed, stopping the helium flow, and the lamp and vacuum pump are switched off. The temperature of evaporator is also set to 5 Celsius again. Then water vapor will condense to water, which can prevent the condensation on the pipes between the evaporator and inter-connecting valve. After the desired temperature is reached, the heat tape and temperature bath are switched off.

The temperature of the evaporator is a key factor for this experiment. If the flow rate of water vapor is lower than the flow rate of helium, adsorption will occur with a water vapor environment of partial water vapor environment, which will lead error to the experiment. If the flow rate of water vapor is much higher than the flow rate of helium, it is possible that water vapor will introduce into the microbalance, which will also lead error to the experiment.

To make sure that there is no condensation in the microbalace system during the experiment and to analyze the effect of buoyancy effect of water vapor flow, a standard platinum wire (0.24mm diameter with 99.99+% purity, Goodfellow Cambridge Limited, England) is placed on the sample bowl for calibration. Because platinum can not adsorb water vapor, it is suitable to simulate the conditions of real experiment. And all the experiments are repeated with the same conditions as that for silica gel water vapor experiments.

CHAPTER 5 RESULTS AND ANALYSIS

Using the system discussed in Chapter 4, Fuji type 'RD' and 'A' silica gel are tested using the experimental procedure discussed previously. Adsorption isotherms and adsorption kinetics obtained from the experiment are also presented. The measurement ranges for the temperature and pressure are from 304K to 358K, and 800Pa to 6000Pa, respectively, which are similar to the operation conditions of an adsorption refrigeration cycle. A total of six isotherms are obtained and compared with the experimental results reported from the C.V.V.P [19] as well as those reported by the adsorption chiller manufacturer [33]. Although several empirical models of isotherms have been analyzed, such as *Henry* and *Tóth'*s model, it is found that the *Tóth's* model or equation is most suitable for covering the full range of behaviors of these isotherms, in particular, the capturing of the asymptotic limit at low temperature isotherm. The correlations of isotherm, fitted using the *Tóth's* equation, are also discussed. At the same time, a simple diffusion model using a sphere model is studied with respect to the measured adsorption kinetics that was obtained during the vapour uptake process at constant temperature. This analysis leads to the correlation for the average adsorption diffusivity and from which, a better understanding of the linear drying force (LDF) model is proposed.

5.1 Adsorption Isotherms

Figures 5.1 and 5.2 show the uptake percentages in kg of adsorbate per kg of adsorbent versus the vapour pressure or adsorption isotherms for type "RD" and "A" silica gel, respectively. As can be seen from Figures 5.1 and 5.2, the experimental data is found to be linear at low pressure range for all isotherms from 304 K to 358K, which compares favourably with the C.V.V.P [19] data in the adsorption operation range. The dot lines in the figures mean the data from manufacture at 323K and 338K.

For low pressure conditions, the present data exhibits a linear behaviour. The adsorption isotherms of both types of silica gels have finite slopes that are proportional to the vapour pressure. As discussed in Chapter 2, such adsorption isotherms are known to follow the *Henry's Law*, where the adsorption onto the silica gel surface increases with vapour pressure. At low temperature and high vapour pressure, saturation phenomenon is observed for isotherms of 304 K and 310 K, and the asymptopic limit is 35% and 40% for type A and RD silica gel, respectively. It is noted that experiments for the asymptotic limit could not be performed as the saturation pressure approaches.

As shown in table 3.1, the thermophysical properties of the two types of silica gel are quite near. However Type 'RD' silica gel has a slightly larger surface area, higher porous structure and higher thermal conductivity than Type 'A' silica gel. Hence, type 'RD' silica gel shows higher uptake characteristics than type 'A'. In addition, the isotherms of the silica gel-water vapour binary system are similar to those of Type I (favourable) isotherm described in Section 2.3.

The amount of adsorbate depends on the nature of the adsorbent, as well as the adsorbent temperature and gas phase pressure. As shown in Figures 5.1 and 5.2, the adsorption percentage for high pressure is higher than that for low pressure for the same temperature. When the gas phase pressure is high, there are more chances for molecules to adsorb onto the adsorbent surface. For a fixed pressure, the adsorption percentage at low temperature is higher than that at high temperature. This is because when the temperature is high, the molecules on the adsorbent surface leave the surface more easily than when there is low temperature, for the same molecular density. This leads to the lower uptake percentage for high temperature than that for low temperature with the same pressure.

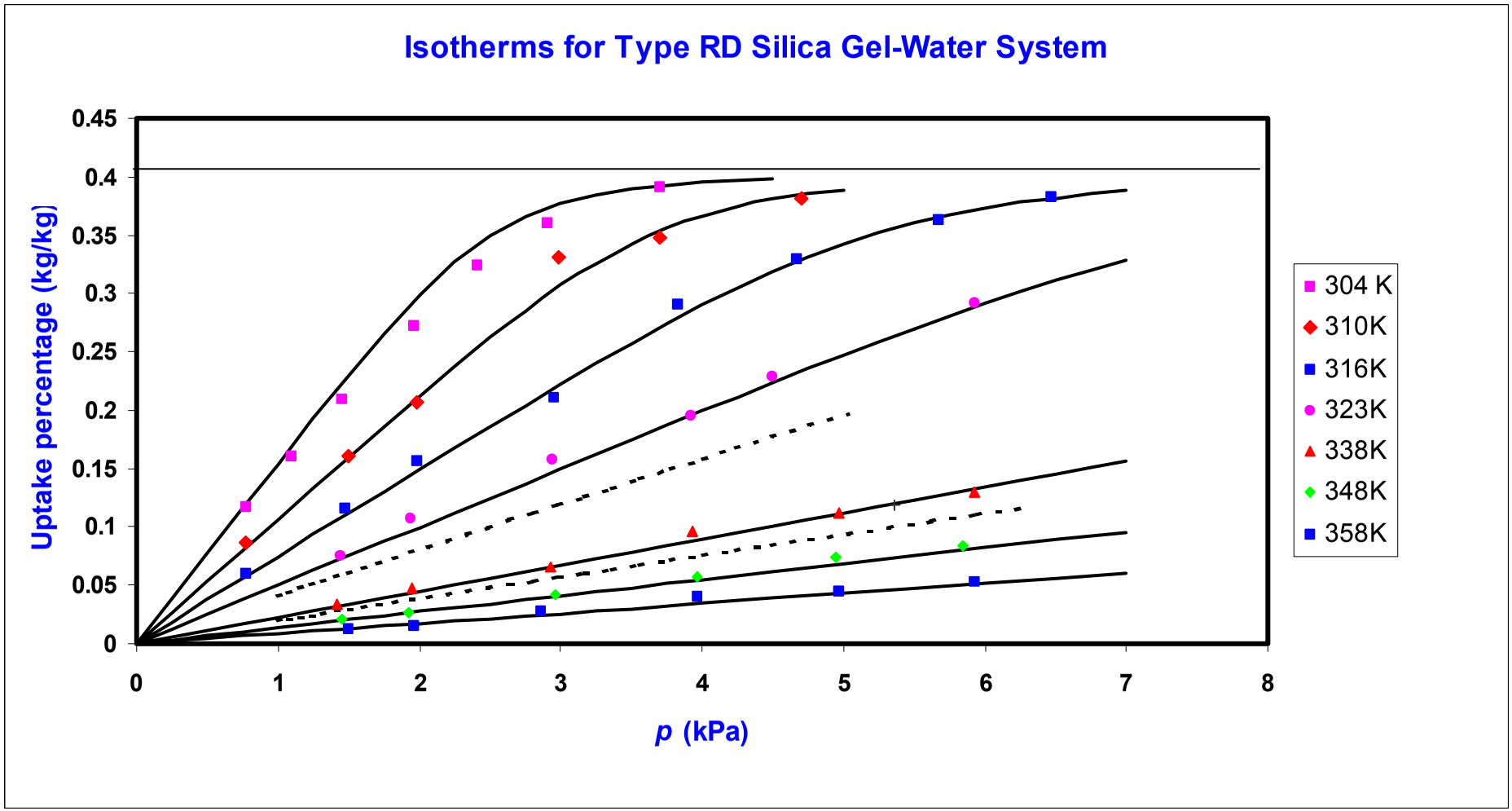

Figure 5.1 Adsorption isotherms of water vapor onto type RD silica gel

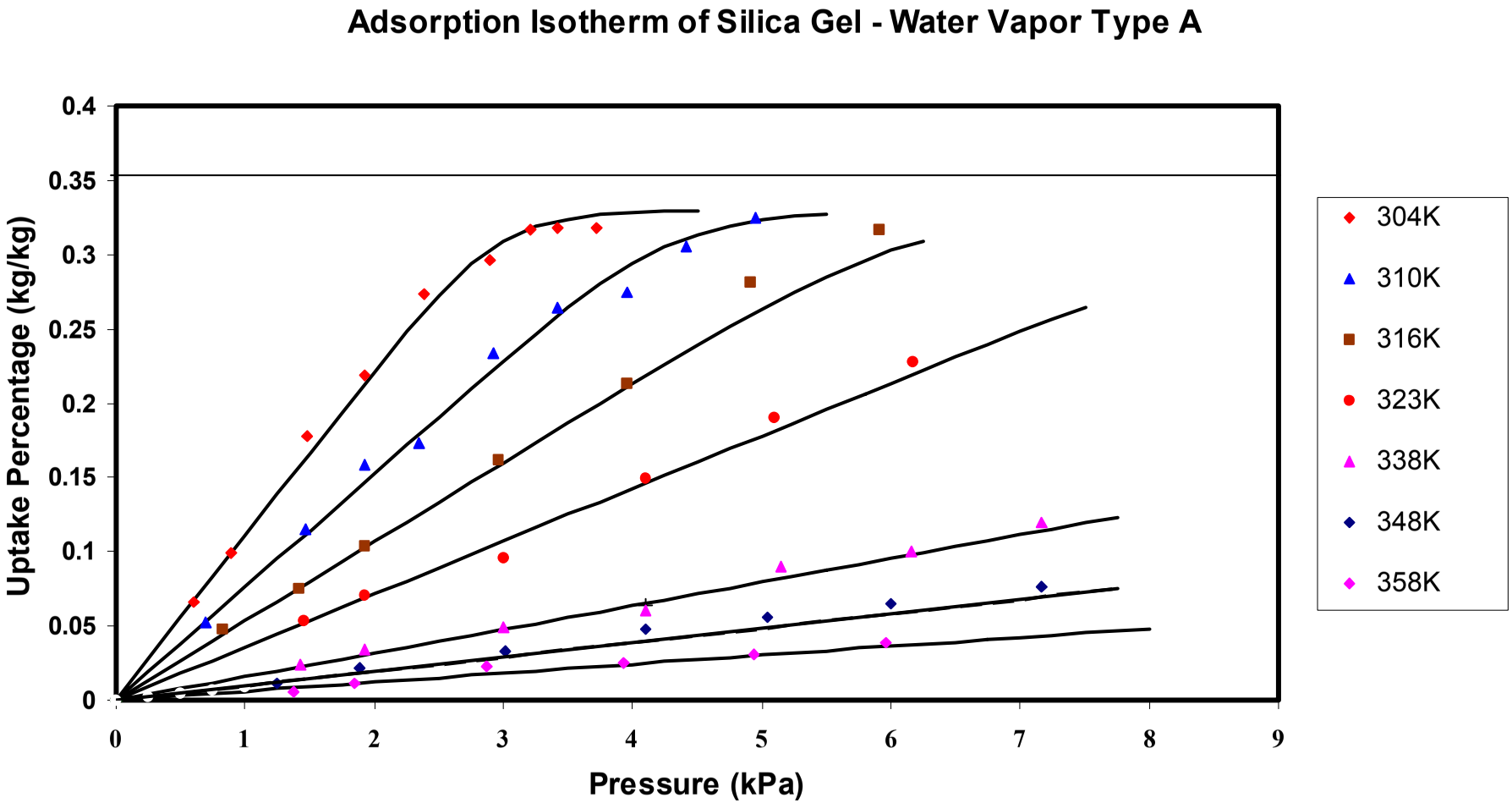

Figure 5.2 Adsorption isotherms of water vapor onto type A silica gel

The amount of silica gel used affects uncertainty in the adsorption measurements. If the sample weight is larger, the experimental uncertainty is lower because it can reduce the effect of buoyancy forces. In our experiments, more than 100mg of silica gel are used for investigation. The detailed computation of experimental uncertainty will be discussed in Section 5.4.

A correlation of experimental data may help us to understand the fundamentals of adsorption. In current experiment, *Tóth's* equation [38] is found to be most suitable for the analyses of experimental data. In the low pressure range, the adsorption constant (K_0) and isosteric heats of adsorption (Q_{st}) can be determined from *Henry's* plot, i.e. the graph of $ln(q/p)$ versus $1/T$. A straight line approximation can be used for the Henry Plot. The gradient is $Q_{st}/R=m$ and the intercept is $lnK_0=c$. Then, the values of K_0 and Q_{st} are tabulated. The *Tóth's* equation has four parameters: $a = K_0$, $b = \exp^{\left(\frac{Q_{st}}{RT}\right)}$, $x = P$, $c = q^*$ and $d = t$. The equation is modelled using the equation below, and the adsorption isotherm parameters and isosteric heats of adsorption are summarized in Table 5.1.

$$y = \frac{a \times b \times x}{\left[1 + \left[\frac{a}{c} \times b \times x\right]^d\right]^{\frac{1}{d}}} \qquad (5.1)$$

where $y = q$; $a = K_0$; $b = \exp^{\left(\frac{Q_{st}}{RT}\right)}$; $x = P$; $c = q^*$; $d = t$

The adsorption capacity of adsorbent (q^*) of silica gel is determined from 304K isotherm.

Table 5.1 Correlation Coefficients For Type RD And Type A Silica Gel

Type	Q_{st}**(kJ/kg)**	K_0**(kPa^{-1})**	R**(kJ/kgK)**	q***(kg/kg)**	t
RD	2693	7.3E-10	0.461917	0.4	6
A	2710	4.65E-10	0.461917	0.33	10

The correlated *Tóth's* equation for *Fuji Davison* on both types of silica gels is presented below:

- *Tóth's* equation for type 'RD' silica gel

$$q = \frac{7.3\times10^{-10}\exp^{\frac{2693}{0.4619T}}P}{\left[1+\left[1.6222\times10^{-9}\exp^{\frac{2693}{0.4619T}}P\right]^{6}\right]^{\frac{1}{6}}} \tag{5.2}$$

- *Tóth's* equation for type 'A' silica gel

$$q = \frac{4.65\times10^{-10}\exp^{\frac{2710}{0.4619T}}P}{\left[1+\left[1.1625\times10^{-9}\exp^{\frac{2710}{0.4619T}}P\right]^{10}\right]^{\frac{1}{10}}} \tag{5.3}$$

5.2 Adsorption Kinetics

During the adsorption experiment, the adsorption isotherms are determined at the equilibrium state. However, the adsorption kinetics can be tracked when the water vapor is introduced into the system. The change of weight of adsorbent is recorded during the uptake. Typical uptake graphs on the adsorption kinetics are shown in Figures 5.3 and 5.4 for type 'RD' and 'A' silica gel, respectively. Based on the diffusion equation in a sphere (discussed in Chapter 2), the experimental data are correlated with different diffusivities. The correlated results at different temperatures

are shown in Figure 5.5 and 5.6 for type 'RD' and 'A' silica gel, respectively. The adsorption diffusivity is found to be higher for high temperature, typically the adsorption diffusivity for type 'RD' at 356 K is about 3 times of that at 304 K. This is because the molecules are easier to be adsorbed and desorbed on a pore surface at high temperature than at low temperature. In current experiments, the pressure ratio variation is small and thus, the average of different diffusivities is found to vary dominantly with the temperatures. From the experiments, it is found that the adsorption rate of type 'RD' silica gel is higher than type 'A' silica gel at the same adsorbent temperature. This is expected since Type 'RD' silica gel has larger surface area and porosity, which dominates the transport of molecules during the experiment.

We propose the adsorption diffusivity of water vapor onto type 'RD' and 'A' silica gel could be characterized by a similar equation discussed in Chapter 2, except for the minor changes to the exponential Poynting factor (F):

$$D_s = D_{so} \exp\left(-\frac{E_a}{RT_b} F \right) \tag{5.4}$$

where D_e is the effective diffusivity, D_{eo} is pre-exponent constant in the kinetics equation, E_a is activation energy of surface diffusion (Refer to Chapter 2), R is universal gas constant, F (effective temperature) is the proposed correction factor based on the temperature of vapour relative to T_b, ie. $F=(T_b/T)^n$. T_b is th^n e triple-point temperature of adsorbate, T is the adsorbent temperature. n is a exponent. For Henry type behavior, the index n is about 0.5.

Table 5.2 Correlation Coefficients For Diffusivity Of Type RD And Type A Silica Gel

Type	D_{so}(m^2/s)	E_a(J/mol)	Q_{st}(kJ/kg)	R(J/mol.K)	T_o (K)	n	a(m)
RD	2.44E-04	4.38E+04	2693	8.314	273.16	0.5	1.7E-04
A	2.54E-04	4.48E+04	2710	8.314	273.16	0.5	1.5E-04

The diffusivity equations for type 'RD' and 'A' silica gels are listed below:

- Diffusivity equation for type 'RD' silica gel

$$D_s = 2.44\times10^{-4}\exp\left(-\frac{4.38\times10^4}{8.314\times273.16\left(\frac{T}{273.16}\right)^{0.5}}\right) \tag{5.5}$$

- Diffusivity equation for type 'A' silica gel

$$D_s = 2.54\times10^{-4}\exp\left(-\frac{4.48\times10^4}{8.314\times273.16\left(\frac{T}{273.16}\right)^{0.5}}\right) \tag{5.6}$$

The goodness of the proposed correlation is shown by colored dots in Figure 5.5 and 5.6 for type 'RD' and 'A' silica gel, respectively. This implies a higher gas temperature, more adsorbate molecules are found to leave the pore surface due to high energy levels of the molecules, leading to lower diffusivity values.

The ratios between activation energy and the isosteric heat of adsorption for type 'RD' and 'A' silica gel are 0.9035 and 0.9184, respectively [6].

Comparing the experimental results for type 'A' silica gel and Suizuki's experiments [3], it is found that the diffusivity from this experiment is about 2 to 3 times larger than that from Suizuki's experiment. Suzuki highlighted that his experimental data were 2 to 3 times lower in values when compared with his proposed correlation. The present experiments with Type 'A' and 'RD' silica gel are in good agreement with his correlation if an effective temperature is employed.

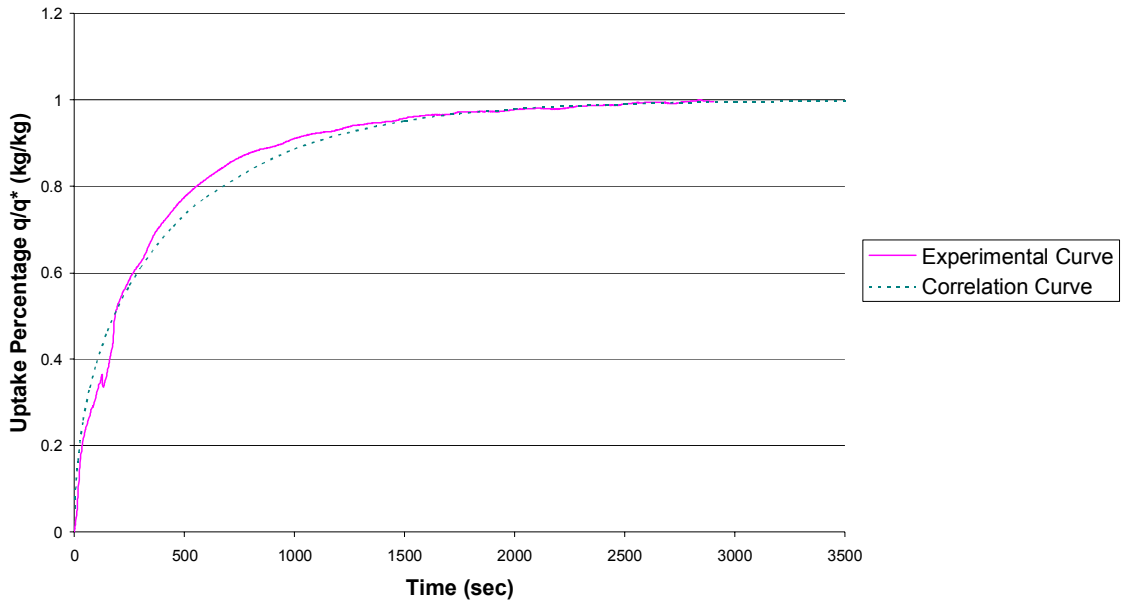

Figure 5.3 Adsorption of water vapor onto type RD silica gel at 43^{o}C 15mbar

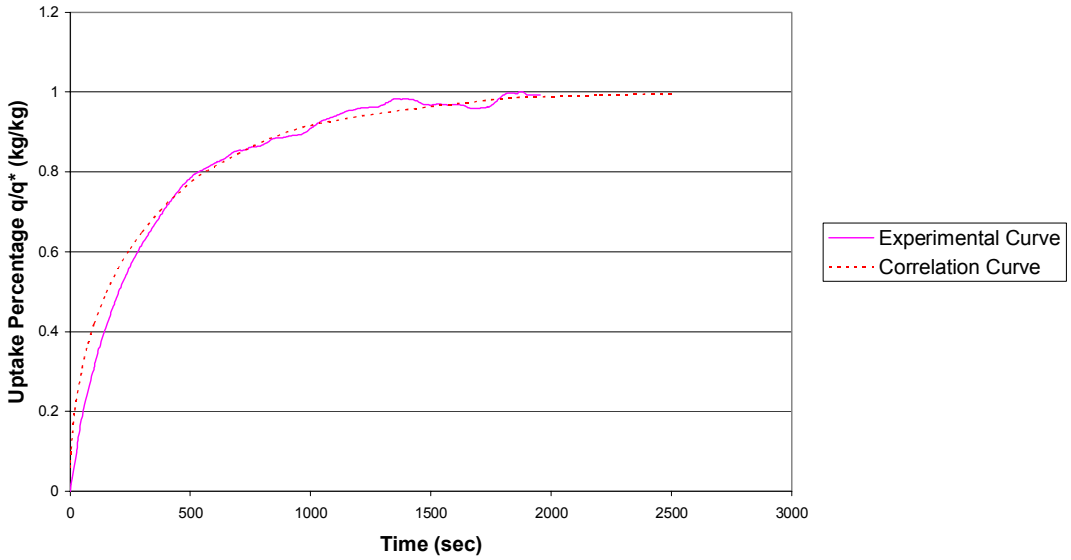

Figure 5.4 Adsorption of water vapor onto type A silica gel at 50^{o}C 20mbar

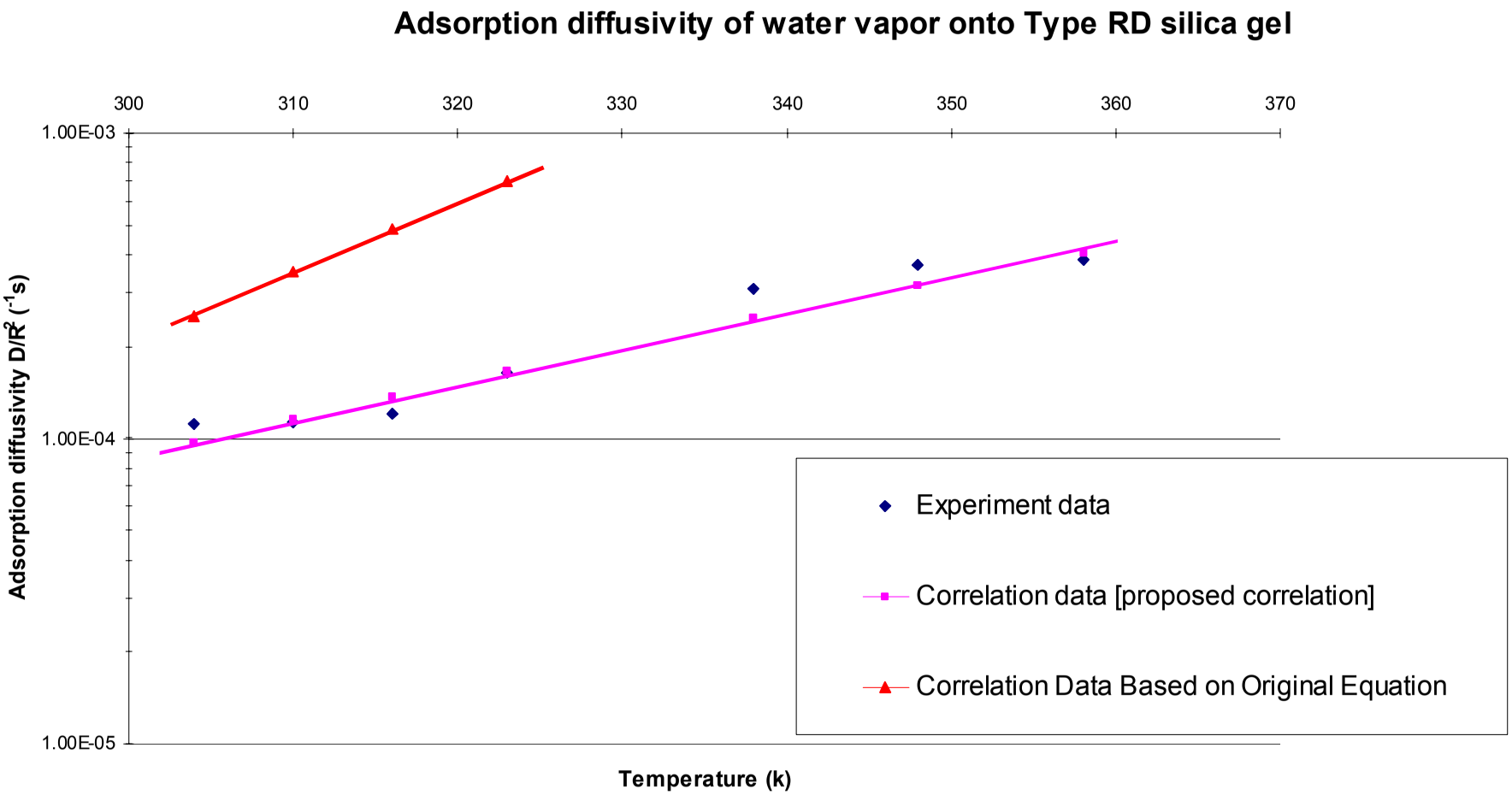

Figure 5.5 Adsorption diffusivity of water vapor onto type RD silica gel

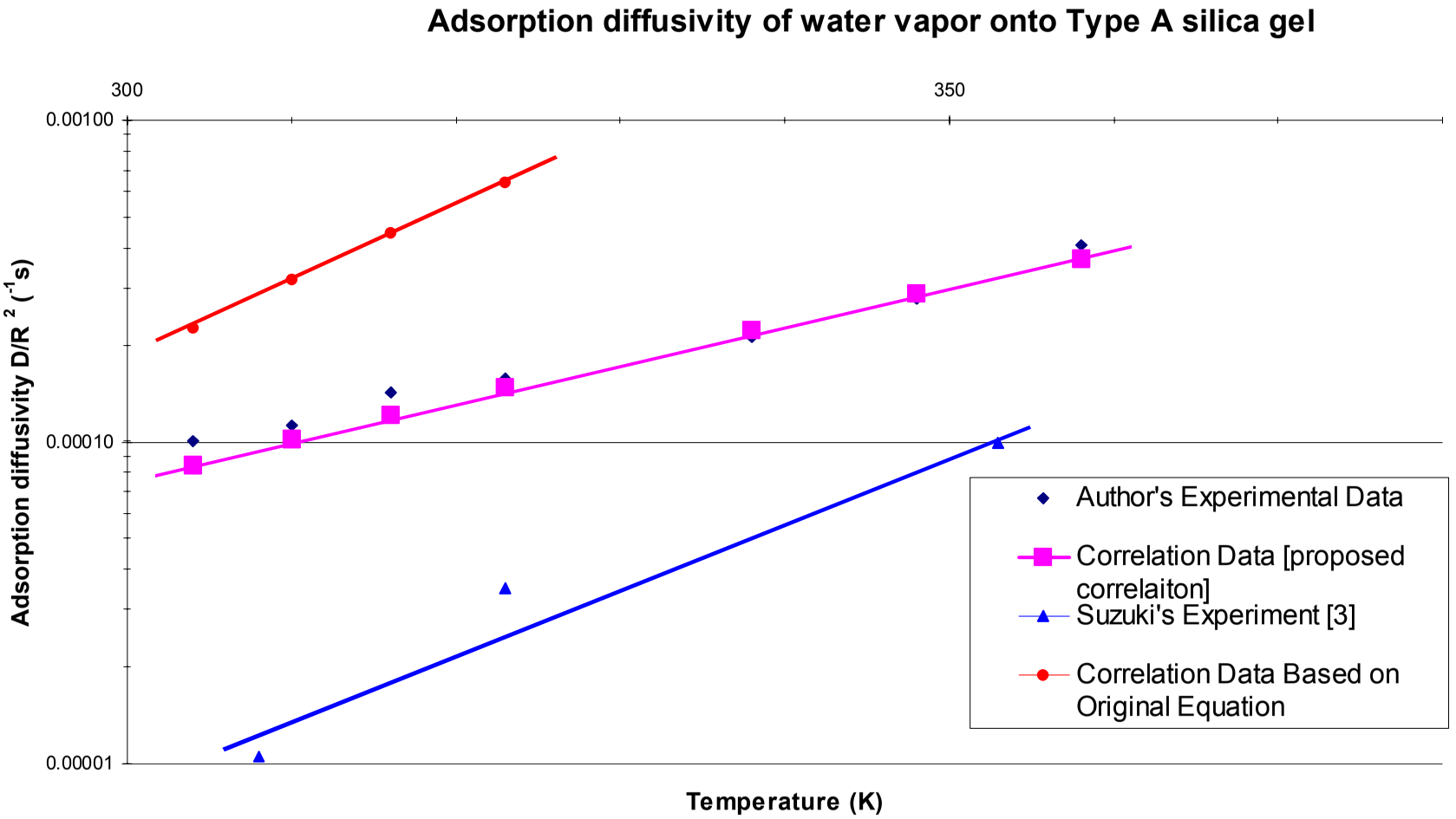

Figure 5.6 Adsorption diffusivity of water vapor onto type A silica gel

5.3 Experiment Calibration

In the calibration experiment, a 123 mg high purity Platinum wire is put in the sample bowl. The experiments are repeated with the same conditions for the adsorption experiments. As shown in Figure 5.7, for pressures less than the saturation pressure, the sample weight will be slightly lower than the true weight of sample because of influence of the buoyancy. On the other hand, when pressure is higher than the saturation pressure at that temperature, there was condensation on the sample. At a temperature of 31 ^{o}C, when the pressure is higher than the saturation pressure, the weight of sample is higher than the real weight of sample. As shown in Figure 5.3, the largest deviation is about 0.4 mg. The largest percentage is thus less than 0.4 per cent.

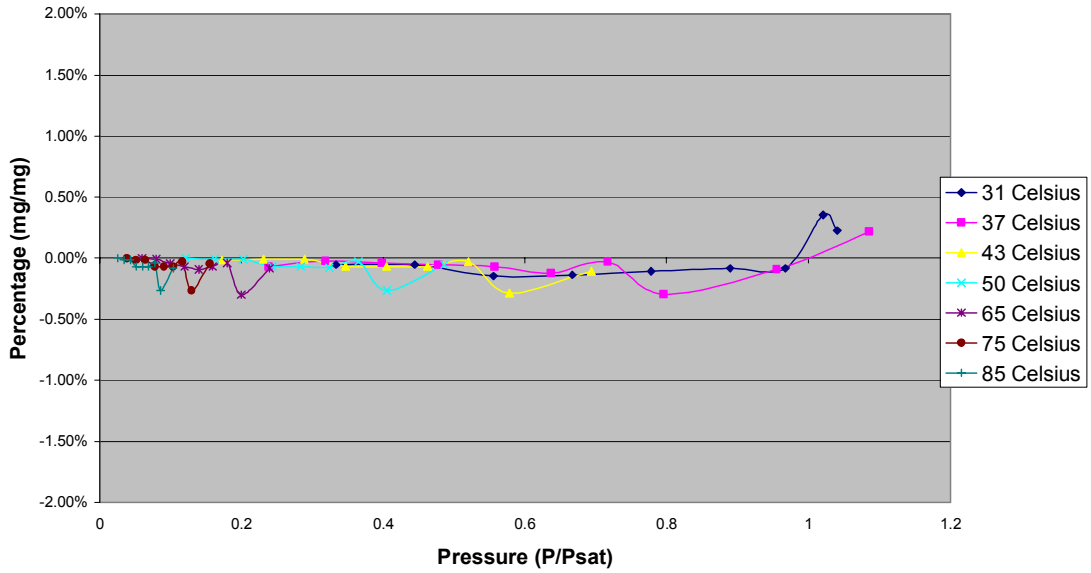

Figure 5.7 Weight deviation calibrated by Platinum

5.4 Error Analysis

The main errors arise from the fluctuation of weight, which is caused by the fluctuation of water vapor flow, dry mass and system deviation. This adsorption experiment is done with the thermogravimetric method, which is a dynamic system.

Buoyancy also resulted in some uncertainty but this is not related to the temperature and pressure of experiment. The fluctuation appears to be affected by the reaction time of the control valve, flow of helium and flow of water vapor.

The adsorption percentage of silica gel can be calculated as follows:

$$q = \frac{m_t - m_{sg}}{m_{sg} + \Delta m_{sys}} \tag{5.6}$$

where q is the uptake percentage, %

m_t is the total mass weight, mg

m_{sg} is the dry mass of silica gel, mg

Δm_{sys} is the system deviation, mg

A formula for $\Delta q/q$, due to experimental errors, was formulated.

$$\frac{\Delta q}{q} = \sqrt{\left(\frac{\sqrt{(\Delta m_t)^2 + (\Delta m_{sg})^2}}{m_t - m_{sg}}\right)^2 + \left(\frac{\sqrt{(\Delta m_{sg})^2 + (\Delta\Delta m_{sys})^2}}{m_{sg} + \Delta m_{sys}}\right)^2} \tag{5.7}$$

It is noted that at high temperatures and low pressures, the experimental uncertainties for the measured isotherms are between 0.6 to 2%. This forms the majority over 90% of the measured points of the experimental data. However, at pressure less than 3 kPa and T higher than 348 K, the maximum experimental uncertainties increase to less than 5%. The increase in the uncertainty is mainly attributed to the low vapour-uptake.

The details of a typical error calculation are shown in Appendix A. From the calculation procedure, the error is found to be mainly caused by the weight difference of silica gel before and after the adsorption. If the weight difference is larger, the error percentage would be smaller. With the current system, the dry mass of sample is normally larger than 100 mg. Thus the amount of dry mass does not play an important role in the error calculation.

CHAPTER 6 CONCLUSIONS AND RECOMMENDATIONS

6.1 Conclusions

- In this thesis, a new adsorption measurement system that can deal with both a condensable vapour and non-condensable gases are designed, tested and commissioned. The system comprises a water vapor delivery generator, a vacuum pumped control system and the TGA. The water vapor is delivered from below of the sample holder whilst a small quantity of an inert gas (helium) is introduced from the top to protect the weighing bridge from any condensation. The novel TGA system has the advantage of high precision in measuring the vapour uptake by the adsorbent and the ease of control of its vacuum environment. This system is proved to be practical in adsorption experiments.
- The adsorption isotherms of water vapor onto silica gel are generated with this new adsorption measurement system. The samples of silica gel are *Fuji Davison* type 'RD' and 'A' silica gel. The measurement ranges for temperature are from 304 K to 358 K and pressure are from 800 Pa to 6000 Pa, respectively. The silica gels can adsorb more water vapor at low temperature than at high temperature. Also type 'RD' silica gel can adsorb more water vapor than type 'A' silica gel under same conditions. The results are compared with the results from the C.V.V.P experiment and the manufacturer of silica gels. The comparison shows that the results are in good consistency with other measurement methods. This also supports the conclusion that the new adsorption measurement system was practical for adsorption measurement with condensable vapor. The *Tóth's* equation was found to best fit the performance of type 'RD' and type 'A' silica gel-water binary system.

- The adsorption diffusivities are measured at the same time while the adsorption isotherms are obtained. The adsorption diffusivities are higher for high temperature than that for low temperature. The diffusivities are compared with those from Suizuki's experiment. It is proven that the diffusivities from my experiments are more accurate in his industrial simulation. The adsorption diffusivities are correlated by the surface diffusion model with some modifications.

6.2 Recommendations

- During the experiment, the baffle inside the reactor tube has two functions: one is to prevent water vapor into microbalance, another one is to protect condensation of water vapor on the hangdown wire. But there is some condensation on the top outside surface of baffle tube if the water vapor temperature is very high. If the amount of liquid water is enough, the water will flow down along the outside surface of baffle tube. The water will drop into the sample bowl. This will lead to errors on measurement. A proposed design of the baffle tube, which can prevent the condensation from dropping into sample bowl, is shown in Figure 6.1.

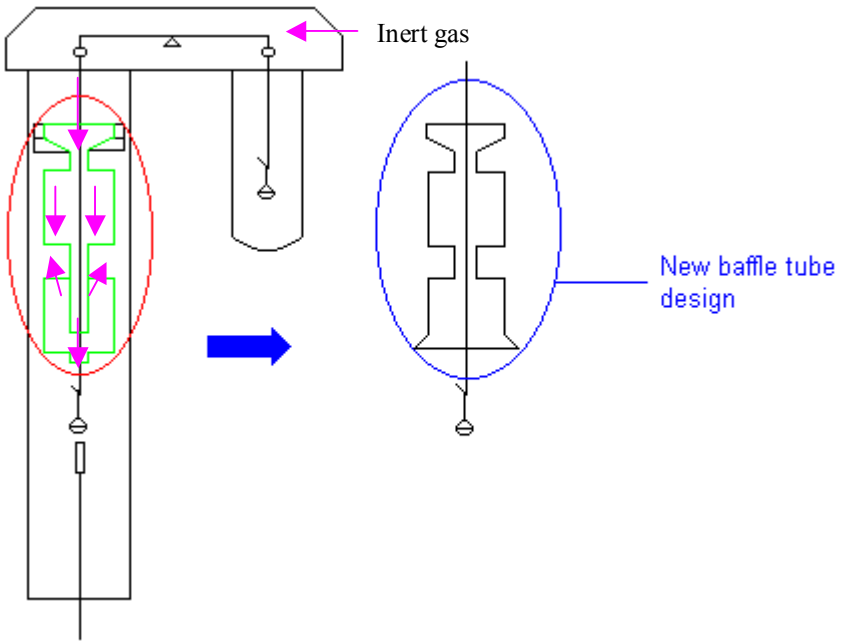

Figure 6.1 Proposed design of baffle tube

❖ For the TGA system, the temperature is measured by the K-type thermocouple, which has a measurement range from 0 K to 423K. The K type thermocouple is not precise enough for the low temperature experiment. In the new design, an additional flexible RTD to coil around the k-type thermocouple was used to measure the accurate temperature of furnace. K type thermocouple still measures and controls the temperature of the furnace, but the more accurate temperature can be recorded by the RTD at the same time. The schematic diagram is shown in Figure 6.2.

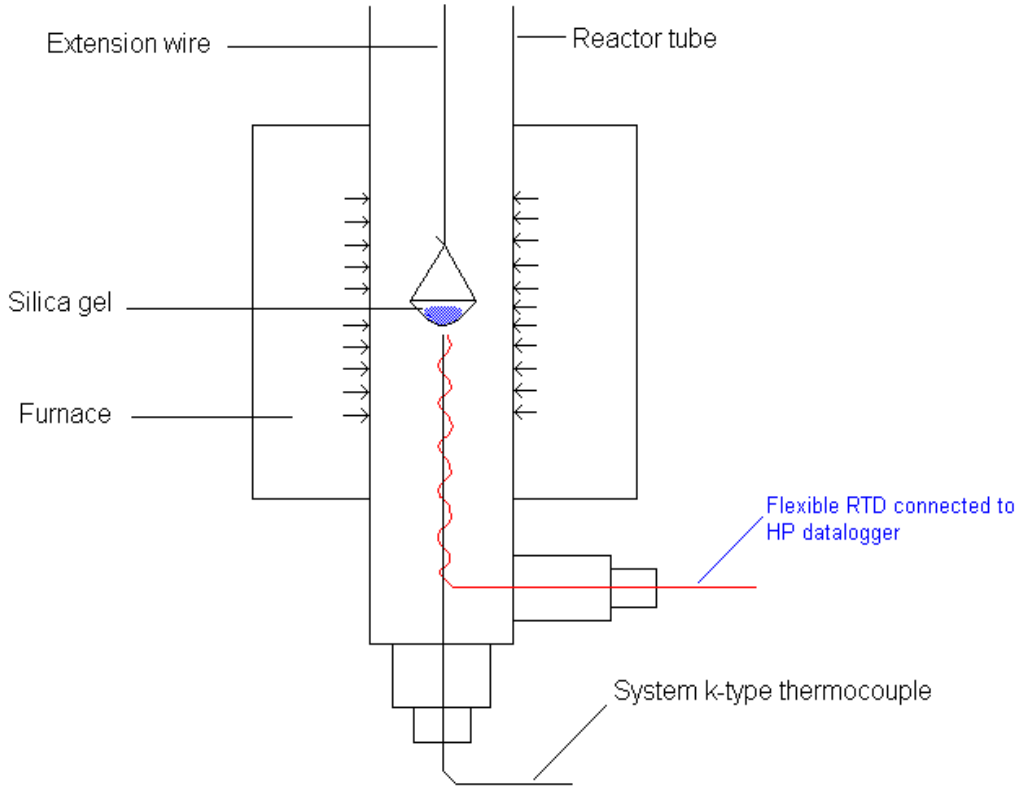

Figure 6.2 Proposed design of flexible RTD

❖ The connection tube between the outlet of reactor tube with the pressure control system is made of Cajon plastic. This tube and its connections are not suitable for

high vacuum experiment. It is suggested to replace this tube and its connection by stainless steel tube and high vacuum connections.

- The temperature of evaporator is not very stable during the experiment. A higher precision temperature controller is recommended to control the temperature of evaporator.

REFERENCES

1. Robens E. J. Rouquerol, F.Rodriguez-Reinoso, K.S.W. Sing and K.K. Unger, Characterization of Porous Solids III, Elsevier, Amsterdam, 1994. p109

2. Douglas M. Ruthven, Shamsuzzaman Farooq and Kent S. Knaebel, Pressure swing adsorption, VCH Publishers , 1994

3. Kazuyuki Chihara and Motoyuki Suzuki, Air drying by pressure swing adsorption, Journal of chemical engineering of Japan, 16(4), 1984

4. Ruthven, D.M. Principles of Adsorption and Adsorption process, John Wiley & Sons, New York, USA, 1984.

5. A.Sakoda and M. Suzuki, Fundamental study on solar powered adsorption cooling system. J Chem Enginnering of Japan, 17 (1), 1984, p52-57.

6. Suzuki, M., "Adsorption Engineering", Elsevier science, New York, 1990, pp. 5-8, 15-16, 35-54.

7. N.C. Srivastava and I.W. Eames, A review of adsorbents and adsorbates in solid-vapour adsorption heat pump systems, Applied thermal engineering, 18, 1998, p707-714.

8. Duong D. Do, "Adsorption analysis : Equilibrica and Kinetics", University of Queensland, January 1998, pp. 1-4, 16-18, 26-27, 64-66.

9. Rouquerol, F., Rouquerol, J. and Sing K., "Adsorption by Powders and Porous Solids : Principles, Methodology and Applications", Academic press, United Kingdom, 1999, pp. 10-11, 18-20.

10. Rong-Luan Yeh, Tushar K. Ghosh, and Anthony L. Hines, "Effects of Regeneration Conditions on the Characteristics of Water Vapour Adsorption on Silica Gel", J. Chem. Eng. Data, 37, 1992, pp. 259-261.

11. User's Manual, "Vapor-generating adapter for CAHN TGA-2121 at ambient pressure or controlled vacuum", Equilibrium vapor pressure version, Thermo Cahn Corporation, 1998.

12. Frank L. Slejko, "Adsorption Technology", 1985, pp.1-4, 9-10.

13. Oscik, J., "Adsorption", Halsted Press, New York, 1982, pp.28-35, 86-88, 102-103.

14. Barry Crittenden, and John Thomas W., "Adsorption Technology and Design", Butterworth-Heinemann, 1997, pp. 1-2, 22, 31-34, 70-74.

15. Mantell C. L., "Adsorption", MCGraw-Hill, New York, 1951, pp.1-2, 20-21, 173.

16. Sing, K. S. W., "Characterisation of Adsorbents", Proc of the NATO Advanced Study Institute on Adsorption – Science and Technology, Vimeiro, Portugal, 1988, pp.3-13, 433.

17. Tien, Chi. Adsorption Calculation and Modeling, Butterworth Heinemann series in Chemical Engineering, 1994.

18. J. Crank, The Mathematics of Diffusion, Oxford University Press, 1975.

19. Chua Hui T., Ng Kim C., Anutosh Chakraborty, Nay M. Oo, and Mohamed A. Othman, "Adsorption Characteristics of Silica Gel + Water Systems", J. Chem. Eng. Data, vol 47, 2002, pp. 1177-1181.

20. A. Sakoda and M. Suzuki, Simultaneous transfport of heat and adsorbate in closed type adsorption cooling system utilizing solar heat, Journal of Solar Engineering, 1986, V108, pp239-245

21. H.T. Chua, K.C.Ng, A. Malek, T. Kashiwagi, A. Akisawa and B.B. Saha, Modeling the performance of two-bed, silica gel-water adsorption chillers, International Journal of Refrigeration, 22(3), 1999, pp194-204.

22. J. Rouquerol and L. Davy, Automatic gravimetric apparatus for recording the adsorption isotherms of gases or vapours onto solids, Thermochimica Acta, 24(2), 1978, p391-397

23. Belal D. and Yuri A., Experimental study on the kinetics of water vapour sorption on selective water sorbents, silica gel and alumina under typical operating conditions of sorption heat pumps, Int. Heat and Mass Transfer, **46**, 2003, pp273-281.

24. Emmett P.H. The measurement of the surface areas of finely divided or porous solids by low temperature adsorption isotherms. Advances in Colloid Science. **1**. 1942, p1-36

25. Rouquerol J.and Davy L., French Patent on device for integral and continuous measurement of gas adsorption and desorption, filed 25/10/1991.

26. Schlosser, E. G. Autometish arbeitende Apparatur zur Oberflächenbestimmung nach BET. Chem. Ing. Tech., 31, 1959, p799.

27. Nelsen F.M. and Eggertsen F.T., Determination of surface area, Adsorption measurements by a continuous flow method Anal. Chem. **30**, 1958, p1387.

28. Website Http://www.cahn.com

29. Website Http://www.rubotherm.com

30. Scott, R. P. W., "Silica Gel and Bonded Phases: Their production, Properties, and use in LC", Wiley, New York, 1993, pp. 78-80.

31. Ofer Sneh, Michelle A. Cameron, Steven M. George, "Adsorption and desorption kinetics of H_2O on a fully hydroxylated SiO_2 surface", Surface Science, 364, 1996, pp. 61-78.

32. Cho, S.H. and J.N. Kim. Modeling of a silica gel/water adsorption-cooling system, Energy, 17(9), 1992, pp. 829-839.

33. Chua, H. T. Universal thermodynamic modelling of chiller: special application to adsorption chillers, Ph.D. thesis, Dept. of Mech. And Prod. Eng., The National University of Singapore, Singapore, 1998.

34. J.M. Gurgel and L.S. Andrade Filho, Thermal diffusivity and adsorption kinetics of silica gel/water, Adsorption, 7, 2001, pp 211-219

35. Cheng-Chin Ni and Jung-yang San, Measurement of apparent solid-side mass diffusivity of a water vapour-silica gel system, International Journal of Heat and Mass Transfer, 45, 2002, pp1839-1847

36. Belal Dawoud and Yuri Aristov, Experimental study on the kinetics of water vapour sorption on selective water sorbents, silica gel and alumina under typical operating conditions of sorption heat pumps, International Journal of Heat and Mass Transfer, 46, 2003, pp273-281

37. HP 34970A Data acquisition / Switch unit, User's Guide, 1997.

38. Toth, J. State equations of the solid-gas interface layers, J. Acta chim. Acad. Sci. Hung. 69, 1971, pp311-328.

39. NACC, PTX data for silica gel/water pair, Manufacturer's Proprietary Data. Nishiodo Air Conditioning Co Ltd.. Tokyo, Japan, 1992

APPENDIX A

CALCULATION FOR EXPERIMENTAL ERRORS

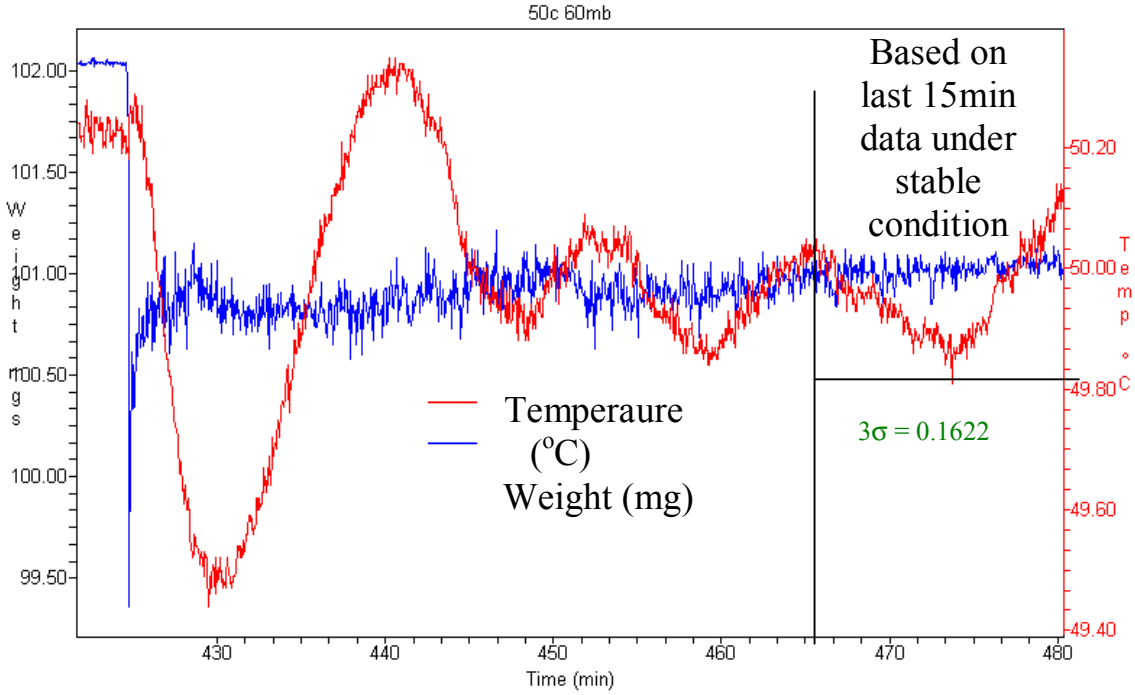

Figure A1 Standard mass weighting deviation at 323K and 6kPa

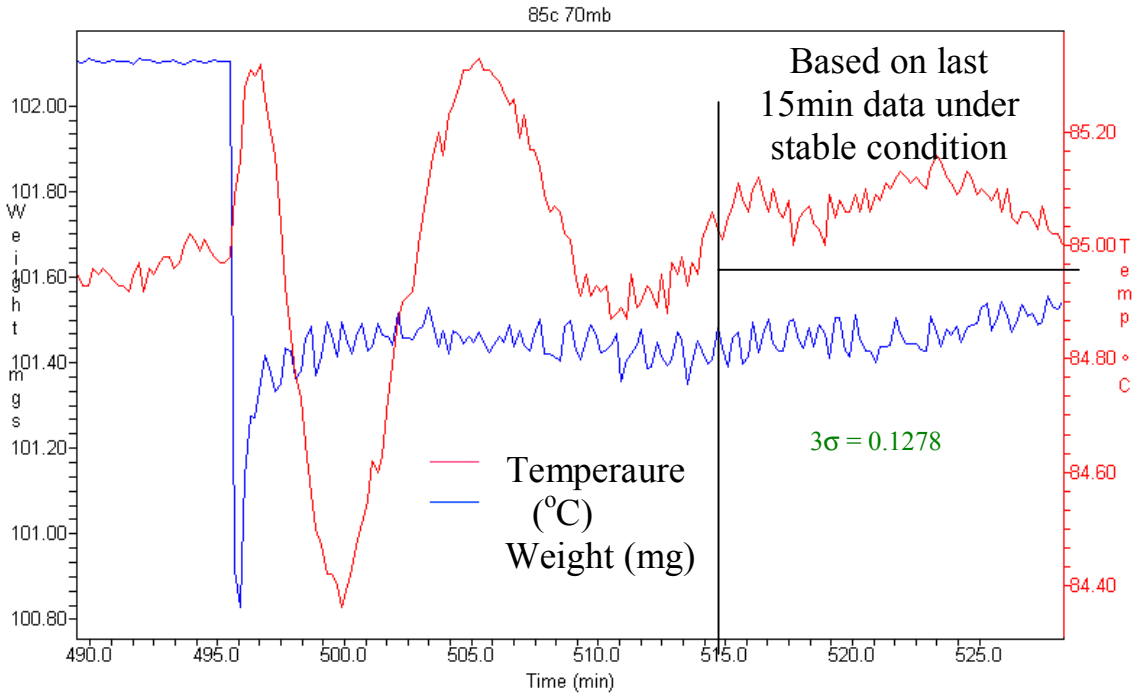

Figure A2 Standard mass weighting deviation at 358K and 7kPa

Calculation for standard deviation (3σ) at 323K and 6kPa

(Based on last 15 minute data)

A	B	C		D	
Time (sec)	Weight (mg)	Temp (°C)		Average weight value (mg)	$(B-D)^2$
27899	100.958	50.04	98.9436	101.0135	0.00308
27902	101.092	50.01	99.0746		0.006162
27905	100.986	50.05	98.9713		0.000756
27908	101.019	50.01	99.0035		3.03E-05
27911	101.02	50.02	99.0045		4.23E-05
27914	100.939	50.04	98.9249		0.00555
27917	101.008	50.02	98.9925		3.02E-05
27920	101.002	50.04	98.9863		0.000132
27923	100.996	50.02	98.9805		0.000306
27926	101.056	50.02	99.0393		0.001806
27929	101.01	50.03	98.9947		1.22E-05
27932	100.916	50.05	98.9024		0.009506
27935	101.098	50.02	99.0803		0.00714
27938	101.026	50.05	99.0097		0.000156
27941	100.909	50.03	98.8952		0.01092
27944	101.009	50.03	98.9935		2.02E-05
27947	100.955	50.03	98.9403		0.003422
27950	101.015	50.01	98.9995		2.25E-06
27953	100.989	49.99	98.9735		0.0006
27956	100.988	50.01	98.9734		0.00065
27959	101.01	50.02	98.9941		1.22E-05
27962	101.002	50.02	98.9863		0.000132
27965	100.991	50.04	98.9762		0.000506
27968	101.039	50.01	99.0234		0.00065
27971	100.903	50.03	98.89		0.01221
27974	100.956	49.99	98.9413		0.003306
27977	101.074	50	99.0572		0.00366
27980	101.031	49.98	99.0156		0.000306
27983	100.882	50.01	98.8688		0.017292
27986	100.912	50.01	98.8982		0.010302
27989	100.961	50	98.9464		0.002756
27992	100.936	50.03	98.9224		0.006006
27995	100.911	50.03	98.8974		0.010506
27998	100.889	50.02	98.8762		0.0155
28001	100.898	50.01	98.8845		0.01334
28004	100.912	50.02	98.8982		0.010302
28007	100.841	49.99	98.8289		0.029756
28010	100.837	49.98	98.8252		0.031152
28013	100.876	49.97	98.8628		0.018906
28016	100.921	49.94	98.9076		0.008556
28019	101.047	49.95	99.0307		0.001122
28022	101.032	49.98	99.0163		0.000342
28025	100.985	49.98	98.9696		0.000812
28028	100.921	49.99	98.9072		0.008556
28031	100.922	49.99	98.908		0.008372
28034	100.942	49.96	98.9275		0.005112

28037	100.979	49.96	98.9645	0.00119
28040	101.118	49.98	99.1004	0.01092
28043	100.998	49.96	98.9832	0.00024
28046	101.039	49.95	99.023	0.00065
28049	101.022	49.93	99.006	7.23E-05
28052	100.932	49.98	98.9177	0.006642
28055	101.009	49.98	98.9936	2.02E-05
28058	101.064	49.96	99.047	0.00255
28061	101.094	49.96	99.0764	0.00648
28064	100.914	49.97	98.9006	0.0099
28067	101.027	49.96	99.0111	0.000182
28070	100.971	49.94	98.9559	0.001806
28073	101.037	49.95	99.0206	0.000552
28076	101.016	49.93	99	6.25E-06
28079	101.043	49.94	99.0264	0.00087
28082	100.953	49.93	98.9386	0.00366
28085	101.044	49.95	99.0282	0.00093
28088	101.003	49.97	98.9881	0.00011
28091	100.988	49.97	98.9728	0.00065
28094	101.036	49.96	99.0203	0.000506
28097	101.087	49.96	99.0697	0.005402
28100	100.946	49.95	98.9315	0.004556
28103	100.958	49.95	98.9438	0.00308
28106	101.056	49.96	99.0394	0.001806
28109	101.091	49.94	99.0737	0.006006
28112	101.008	49.95	98.9926	3.02E-05
28115	101.006	49.96	98.9905	5.62E-05
28118	101.006	49.95	98.9905	5.62E-05
28121	100.98	49.96	98.9654	0.001122
28124	101.004	49.96	98.9884	9.02E-05
28127	101.003	49.97	98.9877	0.00011
28130	101.015	49.95	98.999	2.25E-06
28133	101.006	49.97	98.9906	5.62E-05
28136	101.086	49.95	99.0694	0.005256
28139	101.049	49.99	99.0329	0.00126
28142	101.002	49.99	98.9866	0.000132
28145	101.054	49.96	99.0372	0.00164
28148	101.039	49.97	99.0226	0.00065
28151	100.958	49.95	98.944	0.00308
28154	100.991	49.95	98.9754	0.000506
28157	100.951	49.94	98.9372	0.003906
28160	100.98	49.96	98.9652	0.001122
28163	100.993	49.94	98.9775	0.00042
28166	100.917	49.93	98.9035	0.009312
28169	100.911	49.91	98.8975	0.010506
28172	100.918	49.94	98.9044	0.00912
28175	100.856	49.92	98.8438	0.024806
28178	100.977	49.93	98.9619	0.001332
28181	101.054	49.95	99.0376	0.00164
28184	101.102	49.95	99.0843	0.007832
28187	101.042	49.95	99.0258	0.000812

28190	100.936	49.92	98.9221	0.006006
28193	100.903	49.91	98.8893	0.01221
28196	100.993	49.94	98.9778	0.00042
28199	101.008	49.92	98.9926	3.02E-05
28202	100.994	49.95	98.9788	0.00038
28205	100.962	49.94	98.9472	0.002652
28208	100.997	49.92	98.9822	0.000272
28211	100.997	49.92	98.9815	0.000272
28214	100.964	49.94	98.9497	0.00245
28217	100.887	49.92	98.8744	0.016002
28220	100.92	49.94	98.9065	0.008742
28223	100.939	49.93	98.9252	0.00555
28226	101.058	49.92	99.0413	0.00198
28229	101.092	49.92	99.0752	0.006162
28232	101.047	49.92	99.0307	0.001122
28235	100.983	49.92	98.9683	0.00093
28238	101.025	49.94	99.0097	0.000132
28241	101.001	49.93	98.9852	0.000156
28244	100.999	49.93	98.984	0.00021
28247	100.964	49.91	98.9493	0.00245
28250	101.006	49.89	98.9902	5.62E-05
28253	100.996	49.9	98.9806	0.000306
28256	100.952	49.91	98.9375	0.003782
28259	100.948	49.92	98.9336	0.00429
28262	100.999	49.9	98.9839	0.00021
28265	101.09	49.92	99.0733	0.005852
28268	101.054	49.89	99.0372	0.00164
28271	100.941	49.91	98.9269	0.005256
28274	100.933	49.89	98.9187	0.00648
28277	100.997	49.89	98.9822	0.000272
28280	101.004	49.89	98.9891	9.02E-05
28283	101.011	49.86	98.9959	6.25E-06
28286	101.007	49.88	98.9919	4.22E-05
28289	101.079	49.88	99.0624	0.00429
28292	101.015	49.9	98.9999	2.25E-06
28295	101.007	49.89	98.9916	4.22E-05
28298	101.077	49.89	99.0604	0.004032
28301	101.043	49.88	99.0269	0.00087
28304	100.965	49.88	98.9505	0.002352
28307	100.977	49.89	98.9618	0.001332
28310	101.066	49.87	99.0491	0.002756
28313	101.094	49.87	99.0764	0.00648
28316	101.028	49.88	99.0117	0.00021
28319	101.005	49.89	98.9897	7.22E-05
28322	101.021	49.9	99.0052	5.63E-05
28325	101.019	49.92	99.0031	3.03E-05
28328	101.012	49.91	98.9966	2.25E-06
28331	101.003	49.89	98.9875	0.00011
28334	101.044	49.89	99.0281	0.00093
28337	101.014	49.9	98.9984	2.5E-07
28340	101.048	49.88	99.0314	0.00119

28343	101.033	49.9	99.0169	0.00038
28346	100.923	49.9	98.9096	0.00819
28349	100.846	49.9	98.8333	0.028056
28352	100.849	49.88	98.8369	0.02706
28355	100.895	49.9	98.8822	0.014042
28358	100.963	49.87	98.9487	0.00255
28361	100.963	49.88	98.9488	0.00255
28364	101.018	49.9	99.0028	2.03E-05
28367	101.043	49.89	99.0273	0.00087
28370	101.007	49.91	98.992	4.22E-05
28373	101.017	49.9	99.0015	1.23E-05
28376	101.028	49.88	99.0119	0.00021
28379	101.044	49.88	99.0275	0.00093
28382	101.005	49.87	98.9892	7.22E-05
28385	101.087	49.89	99.0703	0.005402
28388	101.054	49.88	99.0376	0.00164
28391	100.93	49.87	98.9164	0.006972
28394	100.992	49.88	98.9765	0.000462
28397	101.108	49.84	99.0902	0.00893
28400	101.011	49.85	98.9953	6.25E-06
28403	101.014	49.85	98.9989	2.5E-07
28406	101.025	49.85	99.0088	0.000132
28409	100.998	49.87	98.9824	0.00024
28412	101.075	49.89	99.0578	0.003782
28415	101.032	49.87	99.0164	0.000342
28418	101.012	49.89	98.996	2.25E-06
28421	101.013	49.86	98.9977	2.5E-07
28424	100.946	49.81	98.9318	0.004556
28427	101.041	49.85	99.0251	0.000756
28430	101.03	49.87	99.0138	0.000272
28433	100.911	49.85	98.8979	0.010506
28436	101.049	49.86	99.0327	0.00126
28439	101.076	49.87	99.0593	0.003906
28442	100.922	49.86	98.908	0.008372
28445	101.06	49.86	99.0439	0.002162
28448	101.014	49.86	98.9985	2.5E-07
28451	101.028	49.86	99.0123	0.00021
28454	100.978	49.89	98.9636	0.00126
28457	101.003	49.86	98.9873	0.00011
28460	101.034	49.87	99.0177	0.00042
28463	101.021	49.89	99.0052	5.63E-05
28466	101.081	49.88	99.064	0.004556
28469	100.962	49.87	98.9474	0.002652
28472	101.005	49.89	98.9898	7.22E-05
28475	101.021	49.85	99.0055	5.63E-05
28478	100.984	49.87	98.9686	0.00087
28481	101.052	49.9	99.0354	0.001482
28484	101.037	49.88	99.0214	0.000552
28487	101.002	49.9	98.9871	0.000132
28490	101.021	49.87	99.0052	5.63E-05
28493	101.059	49.87	99.0424	0.00207

28496	100.988	49.91	98.9734	0.00065
28499	101.041	49.88	99.0249	0.000756
28502	101.047	49.87	99.0306	0.001122
28505	100.995	49.9	98.9802	0.000342
28508	101.013	49.89	98.9975	2.5E-07
28511	101.018	49.9	99.0027	2.03E-05
28514	100.979	49.91	98.9639	0.00119
28517	101.071	49.91	99.0546	0.003306
28520	100.99	49.91	98.9754	0.000552
28523	101.003	49.9	98.9873	0.00011
28526	101.006	49.89	98.991	5.62E-05
28529	101.039	49.9	99.0232	0.00065
28532	101.012	49.91	98.9965	2.25E-06
28535	101.008	49.92	98.9924	3.02E-05
28538	100.997	49.91	98.982	0.000272
28541	101.007	49.91	98.9915	4.22E-05
28544	101.044	49.9	99.0278	0.00093
28547	101.057	49.89	99.0409	0.001892
28550	101.074	49.9	99.0572	0.00366
28553	101.038	49.92	99.0223	0.0006
28556	101.073	49.91	99.0566	0.00354
28559	101.067	49.93	99.0504	0.002862
28562	101.068	49.93	99.0517	0.00297
28565	101.086	49.93	99.0687	0.005256
28568	101.086	49.95	99.0687	0.005256
28571	101.056	49.95	99.0399	0.001806
28574	101.045	49.97	99.0287	0.000992
28577	101.09	49.97	99.0733	0.005852
28580	101.106	49.97	99.0884	0.008556
28583	101.046	49.98	99.0294	0.001056
28586	101.04	49.99	99.0236	0.000702
28589	100.961	49.99	98.9461	0.002756
28592	101.04	49.98	99.0239	0.000702
28595	100.979	49.98	98.9641	0.00119
28598	101.049	49.98	99.0332	0.00126
28601	100.97	49.99	98.9558	0.001892
28604	101.057	49.96	99.0404	0.001892
28607	100.996	49.99	98.9809	0.000306
28610	100.996	49.98	98.9805	0.000306
28613	101.034	49.98	99.0179	0.00042
28616	101.008	49.98	98.9923	3.02E-05
28619	100.994	50.01	98.979	0.00038
28622	101.015	50	98.9999	2.25E-06
28625	101.039	50	99.0225	0.00065
28628	101.038	49.99	99.0219	0.0006
28631	101.028	49.97	99.0124	0.00021
28634	101.04	49.99	99.0238	0.000702
28637	101.042	49.96	99.0256	0.000812
28640	101.016	49.96	99.0004	6.25E-06
28643	101.066	49.99	99.0498	0.002756
28646	101.022	49.99	99.0065	7.23E-05

28649	101.065	50	99.0481	0.002652
28652	101.066	49.99	99.0498	0.002756
28655	101.033	49.99	99.0166	0.00038
28658	101.071	50.01	99.0539	0.003306
28661	101.078	50.02	99.0614	0.00416
28664	101.057	50.01	99.0404	0.001892
28667	101.063	50	99.0466	0.00245
28670	101.044	50.06	99.0277	0.00093
28673	101.032	50.04	99.0163	0.000342
28676	101.046	50.03	99.03	0.001056
28679	101.085	50.04	99.0683	0.005112
28682	101.068	50.03	99.0515	0.00297
28685	101.061	50.05	99.044	0.002256
28688	101.059	50	99.0423	0.00207
28691	101.061	50.02	99.0445	0.002256
28694	101.051	50.02	99.0349	0.001406
28697	101.048	50.04	99.0315	0.00119
28700	101.048	50.05	99.0316	0.00119
28703	100.996	50.03	98.9805	0.000306
28706	101.074	50.02	99.0576	0.00366
28709	101.044	50.02	99.0277	0.00093
28712	101.011	50.08	98.9952	6.25E-06
28715	101.073	50.08	99.0559	0.00354
28718	101.038	50.05	99.0215	0.0006
28721	100.998	50.05	98.9825	0.00024
28724	101.118	50	99.1004	0.01092
28727	100.977	50.05	98.9622	0.001332
28730	101.051	50.05	99.0348	0.001406
28733	100.999	50.06	98.9838	0.00021
28736	101.065	50.04	99.0485	0.002652
28739	101.095	50.07	99.0776	0.006642
28742	101.051	50.01	99.035	0.001406
28745	101.061	50.05	99.0444	0.002256
28748	101.066	50.06	99.0492	0.002756
28751	101.066	50.03	99.0499	0.002756
28754	101.108	50.06	99.0906	0.00893
28757	101.05	50.06	99.0341	0.001332
28760	101.068	50.08	99.0514	0.00297
28763	101.092	50.07	99.075	0.006162
28766	101.015	50.1	98.9999	2.25E-06
28769	101.026	50.06	99.0099	0.000156
28772	101.055	50.08	99.0386	0.001722
28775	101.042	50.08	99.0261	0.000812
28778	101.045	50.06	99.0285	0.000992
28781	101.053	50.09	99.0366	0.00156
28784	101.029	50.09	99.0132	0.00024
28787	101.137	50.06	99.1194	0.015252
28790	101.032	50.1	99.016	0.000342
28793	101.088	50.11	99.0714	0.00555
28796	101.066	50.1	99.0499	0.002756
28799	101.06	50.14	99.0431	0.002162

28802	101.11	50.1	99.0923		0.009312
28805	101.077	50.12	99.0604		0.004032
28808	100.988	50.12	98.9733		0.00065
28811	101.046	50.14	99.03		0.001056
28814	100.967	50.1	98.9528		0.002162
28817	101.028	50.13	99.0117		0.00021
28820	101.028	50.11	99.0117		0.00021
28823	101.007	50.1	98.9917		4.22E-05
28826	101.029	50.12	99.0129		0.00024
28829	101.049	50.09	99.0327		0.00126
28832	101.004	50.08	98.9882		9.02E-05
28835	101.024	50.07	99.0083		0.00011
28838	101.009	50.09	98.9938		2.02E-05
28841	101.04	50.1	99.024		0.000702
28844	101.048	50.12	99.0317		0.00119
28847	101.036	50.11	99.0197		0.000506
28850	101.046	50.13	99.03		0.001056
				3 sigma (3σ)	**0.162208**

Calculation for standard deviation (3σ) at 358K and 7kPa

(Based on last 15 minute data)

A	B	C		D	
Time (sec)	Weight (mg)	Temp (°C)		Average weight value (mg)	$(B-D)^2$
30905.5	101.391	85.05	99.3015	101.477	0.007396
30917.5	101.459	85.07	99.3685		0.000324
30929.5	101.472	85.11	99.3817		2.5E-05
30941.5	101.398	85.08	99.3088		0.006241
30953.5	101.413	85.06	99.3236		0.004096
30965.5	101.494	85.1	99.4032		0.000289
30977.5	101.423	85.12	99.3329		0.002916
30989.5	101.464	85.09	99.3736		0.000169
31001.5	101.501	85.06	99.41		0.000576
31013.5	101.443	85.1	99.3532		0.001156
31025.5	101.426	85.06	99.3361		0.002601
31037.5	101.427	85.05	99.3374		0.0025
31049.5	101.495	85.08	99.4041		0.000324
31061.5	101.502	85	99.4109		0.000625
31073.5	101.45	85.05	99.3601		0.000729
31085.5	101.433	85.06	99.3434		0.001936
31097.5	101.483	85.07	99.3919		3.6E-05
31109.5	101.439	85.04	99.3486		0.001444
31121.5	101.487	85.03	99.3957		1E-04
31133.5	101.468	85	99.3777		8.1E-05
31145.5	101.41	85.09	99.3201		0.004489
31157.5	101.505	85.05	99.4135		0.000784
31169.5	101.506	85.08	99.4148		0.000841
31181.5	101.427	85.06	99.3372		0.0025
31193.5	101.415	85.06	99.3257		0.003844
31205.5	101.512	85.09	99.4202		0.001225
31217.5	101.453	85.06	99.363		0.000576
31229.5	101.429	85.1	99.3392		0.002304
31241.5	101.428	85.06	99.3383		0.002401
31253.5	101.401	85.09	99.3113		0.005776
31265.5	101.438	85.08	99.3476		0.001521
31277.5	101.436	85.11	99.3463		0.001681
31289.5	101.44	85.1	99.3501		0.001369
31301.5	101.506	85.12	99.4145		0.000841
31313.5	101.468	85.13	99.3777		8.1E-05
31325.5	101.446	85.12	99.3557		0.000961
31337.5	101.444	85.11	99.3538		0.001089
31349.5	101.445	85.12	99.3546		0.001024
31361.5	101.43	85.11	99.3405		0.002209
31373.5	101.428	85.1	99.3382		0.002401
31385.5	101.51	85.14	99.4185		0.001089
31397.5	101.472	85.16	99.3817		2.5E-05
31409.5	101.438	85.15	99.348		0.001521
31421.5	101.479	85.12	99.3886		4E-06
31433.5	101.465	85.11	99.3749		0.000144
31445.5	101.485	85.09	99.3938		6.4E-05

31457.5	101.449	85.1	99.359		0.000784
31469.5	101.481	85.13	99.3905		1.6E-05
31481.5	101.487	85.12	99.3965		1E-04
31493.5	101.492	85.09	99.4005		0.000225
31505.5	101.528	85.1	99.4366		0.002601
31517.5	101.54	85.09	99.4475		0.003969
31529.5	101.475	85.08	99.3838		4E-06
31541.5	101.506	85.1	99.4146		0.000841
31553.5	101.544	85.06	99.4515		0.004489
31565.5	101.507	85.1	99.4159		0.0009
31577.5	101.472	85.05	99.3817		2.5E-05
31589.5	101.501	85.04	99.4101		0.000576
31601.5	101.537	85.06	99.4445		0.0036
31613.5	101.508	85.06	99.4161		0.000961
31625.5	101.516	85.05	99.4249		0.001521
31637.5	101.488	85.03	99.3969		0.000121
31649.5	101.496	85.07	99.4046		0.000361
31661.5	101.555	85.03	99.4627		0.006084
31673.5	101.532	85.02	99.4398		0.003025
31685.5	101.524	85.02	99.4327		0.002209
31697.5	101.542	85	99.4502		0.004225
31709.5	101.51	85.02	99.4181		0.001089
31721.5	101.569	84.93	99.4761		0.008464
31733.5	101.563	84.97	99.4708		0.007396
31745.5	101.483	84.98	99.3925		3.6E-05
31757.5	101.506	84.99	99.4147		0.000841
31769.5	101.52	84.95	99.428		0.001849
31781.5	101.527	84.99	99.4356		0.0025
31793.5	101.532	84.93	99.4396		0.003025
				3 sigma (3σ)	**0.127827**

Calculation for experimental errors

Type RD silica gel

At 358K

P (kPa)	m_t (mg)	m_{sg} (mg)	m_t-m_{sg} (mg)	Δm_{sys} (mg)	$m_{sg}+\Delta m_{sys}$ (mg)	3σ	$\Delta q/q$ (% error)
3	135.62	131.7	3.92	0.45	132.15	0.1278	4.6136
3.913	126.79	122	4.79	1.3	123.3	0.1278	3.7768
4.966	128.07	122	6.07	1.55	123.55	0.1278	2.9818
5.968	128.75	122	6.75	1.6	123.6	0.1278	2.6821
7	139.5	131.7	7.8	1.7	133.4	0.1278	2.3216

At 323K

P (kPa)	m_t (mg)	m_{sg} (mg)	m_t-m_{sg} (mg)	Δm_{sys} (mg)	$m_{sg}+\Delta m_{sys}$ (mg)	3σ	$\Delta q/q$ (% error)
2.975	125	109.6	15.4	0.4	110	0.1622	1.5041
3.913	130.4	109.6	20.8	1.25	110.85	0.1622	1.1221
4.966	136.2	109.6	26.6	1.25	110.85	0.1622	0.8869
5.968	141.88	109.6	32.28	1.25	110.85	0.1622	0.7402
6.998	147.76	109.6	38.16	1.3	110.9	0.1622	0.6357

Type A silica gel

At 358K

P (kPa)	m_t (mg)	m_{sg} (mg)	m_t-m_{sg} (mg)	Δm_{sys} (mg)	$m_{sg}+\Delta m_{sys}$ (mg)	3σ	$\Delta q/q$ (% error)
3.03	161.74	157.5	4.24	0.45	157.95	0.1278	4.2642
4.02	162.8	157.5	5.3	1.3	158.8	0.1278	3.4120
5.16	163.8	157.5	6.3	1.55	159.05	0.1278	2.8711
6.15	164.3	157.5	6.8	1.6	159.1	0.1278	2.6603
7.29	164.8	157.5	7.3	1.7	159.2	0.1278	2.4784

At 323K

P (kPa)	m_t (mg)	m_{sg} (mg)	m_t-m_{sg} (mg)	Δm_{sys} (mg)	$m_{sg}+\Delta m_{sys}$ (mg)	3σ	$\Delta q/q$ (% error)
3	172.5	157.5	15	0.4	157.9	0.1622	1.5361
4.1	180.98	157.5	23.48	1.25	158.75	0.1622	0.9876
5.1	187.43	157.5	29.93	1.25	158.75	0.1622	0.7799
6.17	193.4	157.5	35.9	1.25	158.75	0.1622	0.6551
7	150.9	120	30.9	1.3	121.3	0.1622	0.7661

Remark: $3\sigma = \Delta m_t = \Delta m_{sg} = \Delta\Delta m_{sys}$

(because all are under same condition)

$$3\sigma = 3\left[\frac{\sum_{i=1}^{N}\left(x_i - \overline{x}\right)^2}{N}\right]^{\frac{1}{2}} \qquad \overline{x} = \frac{\sum_{i=1}^{N} x_i}{N}$$

N = no. of items

The data used to compute the 3σ is obtained from Figure E1 and E2 (refer to the previous page)

APPENDIX B

EXPERIMENTAL DATA ON ISOTHERMS AND ADSORPTION RATES

Table B1 Uptake Percentage Of Type RD Silica Gel

304K	Pressure (Kpa)	0.77	1.1	1.45	1.96	2.9	3.7	2.41	
	Uptake Percentage (kg/kg)	0.1167	0.1602	0.2099	0.2720	0.3599	0.3920	0.3245	
310K	Pressure (Kpa)	0.77	1.5	1.98	2.98	3.7	4.7		
	Uptake Percentage (kg/kg)	0.0872	0.1602	0.2064	0.3313	0.3478	0.3810		
316K	Pressure (Kpa)	0.77	1.47	1.98	2.95	3.83	4.67	5.67	6.47
	Uptake Percentage (kg/kg)	0.0604	0.1160	0.1570	0.2117	0.2907	0.3302	0.3638	0.3830
323K	Pressure (Kpa)	1.44	1.94	2.94	3.92	4.5	5.93		
	Uptake Percentage (kg/kg)	0.0752	0.1081	0.1572	0.1956	0.2296	0.2915		
338K	Pressure (Kpa)	1.42	1.95	2.93	3.93	4.97	5.93		
	Uptake Percentage (kg/kg)	0.0342	0.0470	0.0663	0.0960	0.1123	0.1305		
348K	Pressure (Kpa)	1.45	1.92	2.96	3.96	4.95	5.85		
	Uptake Percentage (kg/kg)	0.0215	0.0272	0.0424	0.0572	0.0735	0.0842		
358K	Pressure (Kpa)	1.5	1.96	2.86	3.96	4.97	5.92		
	Uptake Percentage (kg/kg)	0.0129	0.0149	0.0284	0.0402	0.0448	0.0527		

Table B2 Uptake Percentage Of Type A Silica Gel

304K	Pressure (Kpa)	0.6	0.89	1.92	1.48	2.38	2.9	3.21	3.42	3.72	
	Uptake Percentage (kg/kg)	0.0667	0.0991	0.2193	0.1776	0.2734	0.2965	0.3167	0.3179	0.3181	
310K	Pressure (Kpa)	0.7	1.47	1.92	2.34	2.92	3.42	3.96	4.41	4.95	0.7
	Uptake Percentage (kg/kg)	0.0524	0.1147	0.1583	0.1737	0.2340	0.2649	0.2741	0.3050	0.3248	0.0524
316K	Pressure (Kpa)	0.82	1.42	1.92	2.96	3.95	4.91	5.91			
	Uptake Percentage (kg/kg)	0.0476	0.0751	0.1039	0.1615	0.2132	0.2811	0.3172			
323K	Pressure (Kpa)	1.46	1.92	3	4.1	5.1	6.17				
	Uptake Percentage (kg/kg)	0.0541	0.0708	0.0952	0.1491	0.1900	0.2279				
338K	Pressure (Kpa)	1.43	1.93	3	4.1	5.15	6.163	7.17			
	Uptake Percentage (kg/kg)	0.0244	0.0343	0.0493	0.0603	0.0905	0.1003	0.1194			
348K	Pressure (Kpa)	1.25	1.88	3.01	4.1	5.04	6	7.17			
	Uptake Percentage (kg/kg)	0.0117	0.0215	0.0336	0.0476	0.0559	0.0654	0.0762			
358K	Pressure (Kpa)	1.37	1.85	2.87	3.93	4.94	5.96				
	Uptake Percentage (kg/kg)	0.0061	0.0112	0.0232	0.0248	0.0309	0.0386				

Table B3 Adsorption Diffusivity Of Type RD Silica Gel With Water

Uptake Percentage (kg/kg) at 358K	0.0129	0.0149	0.0284	0.0402	0.0448	0.0527			
Adsorption diffusivity ($^{-1}$s)	0.0004	0.0004	0.0003	0.00035	0.00041	0.0004		Average Diffusivity ($^{-1}$s)	0.00039
Uptake Percentage (kg/kg) at 348K	0.0215	0.0272	0.0424	0.0572	0.0735	0.0842			
Adsorption diffusivity ($^{-1}$s)	0.0004	0.0004	0.0003	0.00042	0.00032	0.0004		Average Diffusivity ($^{-1}$s)	0.00037
Uptake Percentage (kg/kg) at 338K	0.0342	0.0470	0.0663	0.0960	0.1123	0.1305			
Adsorption diffusivity ($^{-1}$s)	0.0005	0.0004	0.0003	0.00028	0.00024	0.0002		Average Diffusivity ($^{-1}$s)	0.00031
Uptake Percentage (kg/kg) at 323K	0.0752	0.1081	0.1572	0.1956	0.2296	0.2915			
Adsorption diffusivity ($^{-1}$s)	0.0002	0.0002	0.0002	0.00015	0.0001	0.0001		Average Diffusivity ($^{-1}$s)	0.00016
Uptake Percentage (kg/kg) at 316K	0.1160	0.1570	0.2117	0.2907	0.3302	0.3638	0.3830		
Adsorption diffusivity ($^{-1}$s)	0.0002	0.0001	0.0001	0.0001	0.00008	0.0001	0.0001	Average Diffusivity ($^{-1}$s)	0.00012
Uptake Percentage (kg/kg) at 310K	0.1602	0.2064	0.3313	0.3478	0.3810				
Adsorption diffusivity ($^{-1}$s)	0.0002	9E-05	9E-05	8.8E-05	0.00014			Average Diffusivity ($^{-1}$s)	0.00011
Uptake Percentage (kg/kg) at 304K	0.1602	0.2720	0.3599	0.3920					
Adsorption diffusivity ($^{-1}$s)	0.0002	0.0002	9E-05	0.00009				Average Diffusivity ($^{-1}$s)	0.00011

Table B4 Adsorption Diffusivity Of Type A Silica Gel With Water

Uptake Percentage (kg/kg) at 358K			0.0336	0.0476	0.0559	0.0654	0.0762			
Adsorption diffusivity ($^{-1}$s)			0.0004	0.0004	0.00035	0.00042	0.00044		Average Diffusivity ($^{-1}$s)	0.00041
Uptake Percentage (kg/kg) at 348K			0.0336	0.0476	0.0559	0.0654				
Adsorption diffusivity ($^{-1}$s)			0.0004	0.0004	0.00042	0.00042			Average Diffusivity ($^{-1}$s)	0.00028
Uptake Percentage (kg/kg) at 338K		0.0343	0.0493	0.0603	0.0905	0.1003				
Adsorption diffusivity ($^{-1}$s)		0.00013	0.0001	0.0001	0.00013	0.0001			Average Diffusivity ($^{-1}$s)	0.000213
Uptake Percentage (kg/kg) at 323K	0.0541	0.0708	0.0952	0.1491	0.1900	0.2279				
Adsorption diffusivity ($^{-1}$s)	0.00035	0.00022	0.0001	8E-05	0.00011	8.5E-05			Average Diffusivity ($^{-1}$s)	0.000158
Uptake Percentage (kg/kg) at 316K	0.0751	0.1039	0.1615	0.2132	0.2811	0.3172				
Adsorption diffusivity ($^{-1}$s)	0.0002	0.0002	0.0001	8E-05	0.00012	0.00013			Average Diffusivity ($^{-1}$s)	0.000142
Uptake Percentage (kg/kg) at 310K	0.1147	0.1583	0.1737	0.2340	0.2649	0.2741	0.3050	0.3248		
Adsorption diffusivity ($^{-1}$s)	0.00013	0.00013	0.0001	0.0001	9.5E-05	0.00011	8.5E-05	0.00012	Average Diffusivity ($^{-1}$s)	0.000113
Uptake Percentage (kg/kg) at 304K	0.0991	0.1776	0.2193	0.2734	0.2965	0.3167	0.3179			
Adsorption diffusivity ($^{-1}$s)	0.00015	0.00016	0.0001	7E-05	0.00006	0.00007	0.0001		Average Diffusivity ($^{-1}$s)	0.000101